Liquid Crystals
Publication details, including instructions for authors and subscription information:
http://www.informaworld.com/smpp/title~content=t713926090

Structure-property investigation of 2- and 3-thienylacrylates bearing laterally fluorinated azobenzene moieties

A. S. Matharu[a]; D. Chambers-Asman[b]
[a] Department of Chemistry, University of York, Heslington, UK [b] Division of Chemistry, Nottingham Trent University, Nottingham NG11 8NS, UK

To cite this Article Matharu, A. S. and Chambers-Asman, D.(2007) 'Structure-property investigation of 2- and 3-thienylacrylates bearing laterally fluorinated azobenzene moieties', Liquid Crystals, 34: 11, 1317 — 1336
To link to this Article: DOI: 10.1080/02678290701697447
URL: http://dx.doi.org/10.1080/02678290701697447

Liquid Crystals, Vol. 34, No. 11, November 2007, 1317–1336

Structure–property investigation of 2- and 3-thienylacrylates bearing laterally fluorinated azobenzene moieties

A. S. MATHARU*† and D. CHAMBERS-ASMAN‡

†Department of Chemistry, University of York, Heslington, York YO10 5DD, UK
‡Division of Chemistry, Nottingham Trent University, Nottingham NG11 8NS, UK

(*Received 10 July 2007; accepted 21 September 2007*)

The synthesis, transition temperatures and structure–property relationships of a variety of thiophene-containing azobenzene esters derived from either 3-(2-thienyl)acrylic acid (series **I**, **IV**, **VI**, **VIII**, **X** and **XII**) or 3-(3-thienyl)acrylic acid (series **II**, **V**, **VII**, **IX**, **XI** and **XIII**) and appropriate fluoro- and non-fluoro-substituted 'azophenols' are reported. For comparative purposes, the non-heterocyclic counterparts, i.e. cinnamates (series **III**), were also prepared and are reported. All 70 final esters are mesomorphic, exhibiting the nematic phase alone. Their mesomorphic properties are dependent on the disposition of the terminal thiophene moiety. In general, 3-thienyl-substitution gives thermally more stable compounds than 2-thienyl-substitution. The influence of mono- (series **IV**, **V**, **VI** and **VII**) and di-lateral (series **VIII**, **IX**, **X**, **XI**, **XII** and **XIII**) fluoro-substitution on mesomorphic properties is investigated in detail. Lateral fluorination lowers mesophase thermal stability and its extent is dependent on the number and disposition of the lateral fluoro-substituents. Di-lateral fluorination across the long molecular axis is more detrimental to mesophase thermal stability than along the long molecular axis.

1. Introduction

Structure–property relationships form an important part of the understanding of any applied scientific subject. In the early part of the 20th century, Vorländer developed the origins of structure–property relationships in liquid crystals introducing the concept of a lath-like geometry [1, 2]. This classical calamitic molecular architecture is now the workhorse in the elucidation of many structure–property relationships. Today we are able to design and synthesize liquid crystals with specific structures and functions by manipulating the chemical entities forming the whole construct.

Liquid crystals derived from thiophene, a five-member heterocycle comprising sulfur, are interesting because they deviate from the classical calamitic structure inducing looser packing and thus lowering the melting point. The electronegative sulfur atom imparts a transverse dipole and the ring itself is a rich source of polarizable electrons, which may be useful for electro-optic applications [3, 4]. Thiophene is π-excessive (contains six electrons delocalized over five nuclei) and readily undergoes electrophilic substitution at the α positions (C-2 and C-5) in preference to the β positions (C-3 and C-4). The α di-substitution pattern gives an exocyclic bond angle of 148°, which is intermediate to the angles found in 1,4-phenylene (180°) and 1,3-phenylene (120°) di-substitution:

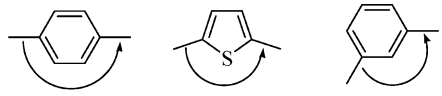

1,4-phenylene 180° 2,5-thienyl 148° 1,3-phenylene 120°

Following initial studies by Schubert *et al.* [5] on the use of thiophene as a mesogenic unit, we have exploited the chemistry of thiophene to good effect to show that, despite its non-linearity, a bend or kink can still be accommodated to produce liquid crystals with reduced melting and clearing points compared with their non-heterocyclic counterparts [6–10].

In our continuing quest to further develop our knowledge of thiophene-based liquid crystals and influence of their structure on mesomorphic properties we now report our results of a systematic study of 2- and 3-thienylacrylates comprising laterally fluorinated azobenzene moieties. Both lateral fluorination and azobenzenes are interesting in their own right. Lateral fluorination is known to lower the melting point, promote nematic phase formation at the expense of high-order smectic phases and influence the sign of the

*Corresponding author. Email: am537@york.ac.uk

Liquid Crystals
ISSN 0267-8292 print/ISSN 1366-5855 online © 2007 Taylor & Francis
http://www.tandf.co.uk/journals
DOI: 10.1080/02678290701697447

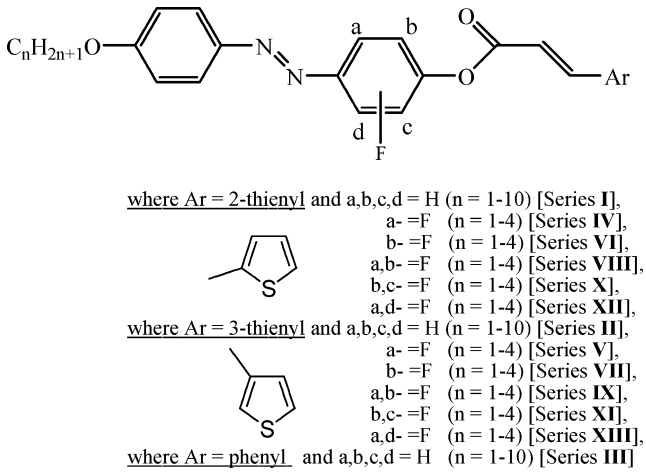

Figure 1. Structures of 2- and 3-thienylacrylates (series **I**, **II**, **IV**–**XIII**) and their non-heterocyclic counterpart (series **III**).

dielectric anisotropy [11, 12]. The latter azobenzene moiety is an important photoresponsive moiety, which has been exploited in controlling the surface alignment and anchoring of liquid crystals via the concept of a 'command surface', optical modulation of the mesophase transitions, and in holographic optical data storage (for a review on optical switches and memories, see [13]). However, it is important to note that photoregulation is outside the scope of this paper; rather, we investigate the influence of structural composition on mesomorphic properties.

In our investigation we have tethered thiophene at one end of the molecule to initially gauge the influence of replacing a terminal phenyl ring (series **III**) with either 2- or 3-substituted thiophene (series **I** and **II**, respectively). See figure 1.

The influence of the alkyl versus alkoxy chain could also be compared since on reviewing the literature we found that Nabeshima *et al* [14] have reported the alkyl-compounds of series **I**. The influence of lateral fluorination is undertaken via a systematic study of monofluoro- and difluoro-substituted 2- and 3-thienylacrylates, where the fluoro-substituents are located on the azobenzene appendage (series **IV**–**XIII**).

2. Results and discussion

2.1. *Synthetic overview*

The synthesis of members of a variety of thiophene-containing azobenzene esters (series **I**, **II**, **IV**–**XIII**) and their non-heterocyclic counterparts (series **III**) is generalized scheme 1.

Commercial 4-nitrophenol (**1**) was alkylated with appropriate 1-bromoalkanes to yield a series of 4-*n*-alkoxynitrobenzenes (**2a**–**j**) in moderate yields (55%). Room-temperature catalytic hydrogenation (10% Pd/C) at either atmospheric or reduced pressure of an ethanolic solution of compounds (**2a**–**j**) gave the desired 4-*n*-alkoxyanilines (**3a**–**j**) in good yields (75–82%). The higher homologues were isolated as hydrochloride salt, whereas the lower homologues were purified by vacuum distillation. Diazotization (concentrated HCl/$NaNO_2$) of the corresponding 4-*n*-alkoxyanilines (**3a**–**j**) followed by treatment with a solution of phenol in 4 M NaOH furnished the appropriate 4-(4-*n*-alkoxyphenylazo)-phenols (**4a**–**j**, **5a**–**j**, **6a**–**j**, **7a**–**j**, **8a**–**j**, **9a**–**j**). The *para*-isomer (45%) was predominantly formed and since purity is essential, the compounds were rigorously purified by flash column chromatography followed by repeated recrystallization. The final esters were prepared using the DCC esterification procedure because it is a room-temperature, high-yielding, one-pot reaction [15].

2.2. *Synthetic procedures*

For the sake of brevity, only salient synthetic details are given in this section. The structural integrity of the intermediates and final products was evidenced by ^{1}H nuclear magnetic resonance (NMR) spectroscopy (JEOL FX60Q 270 MHz spectrometer) with tetramethylsilane as the internal standard and infrared spectroscopy (Perkin-Elmer FT1605 spectrophotometer). High-resolution mass spectrometry (HRMS) was performed using a Bruker Daltronics micrOTOF spectrometer. The experimental details for the preparation of 4-*n*-alkoxyanilines (**3a**–**j**) from the corresponding 4-*n*-alkoxynitrobenzenes (**2a**–**j**) are well documented and can be found in [16, 17]. For each series, full characterization is only given for one homologue, which serves as a good representative for the remaining members of that series.

2.2.1. General method for diazotization and coupling: 4-(4-*n*-alkoxyphenylazo)phenols (4a–j); 4-(4-*n*-alkoxyphenylazo)fluorophenols (e.g. 5a–j, 6a–j) and; 4-(4-*n*-alkoxyphenylazo)difluorophenols (e.g. 7a–j, 8a–j, 9a–j). A cooled (0°C) solution of sodium nitrite (1.0 g, 15 mmol) in water (50 ml) was added to a cooled solution/suspension of the appropriate 4-*n*-alkoxyaniline (e.g. **3a**–**j**; 15 mmol) in HCl/water (5.4 ml:27 ml). The reaction mixture was maintained at 0°C for 2 h to ensure successful diazotization. Thereafter, a mixture of phenol (1.4 g, 15 mmol) or appropriate 'fluorophenol' (15 mmol), sodium hydroxide (1.8 g, 45 mmol) and water (40 ml) was added, dropwise, with stirring to the above diazonium solution ensuring that the reaction temperature did not exceed 5°C. After stirring for 2 h, the ensuing orange precipitate was filtered (Büchner) and transferred into a

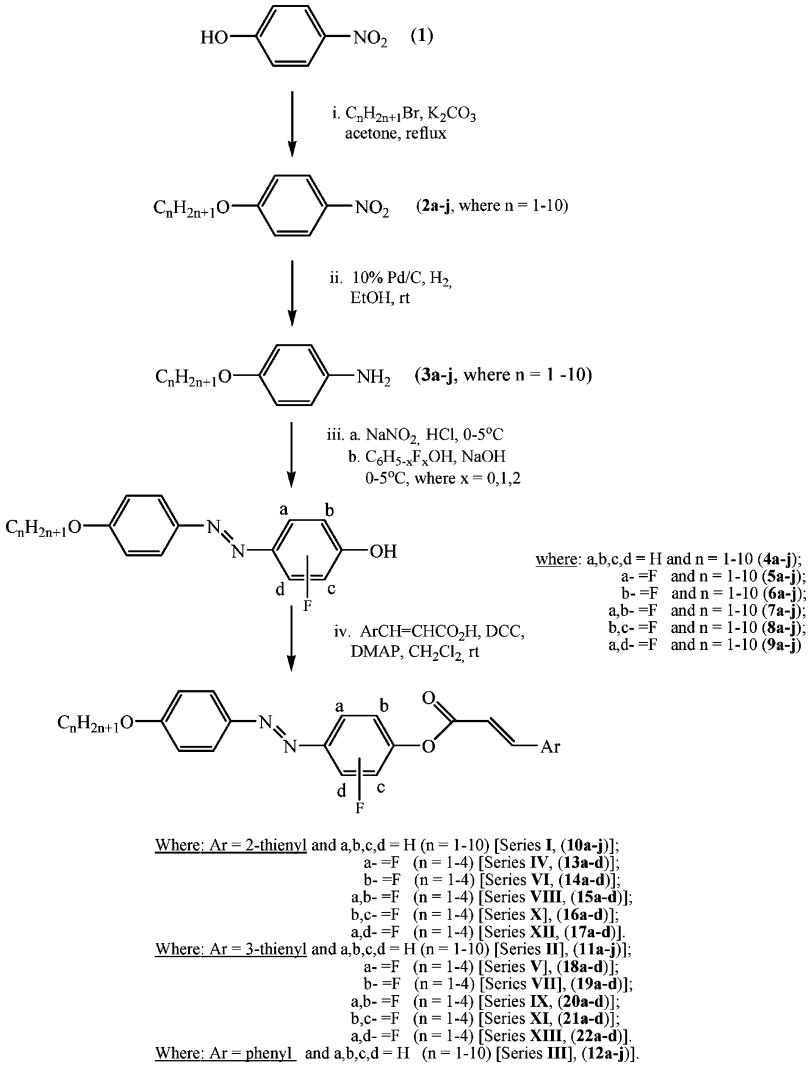

Scheme 1. Generalized pathway for the synthesis of a variety of fluoro- and non-fluoro-substituted azobenzene-containing acrylates, i.e. series **I**–**XIII**.

separating funnel containing CH_2Cl_2 (100 ml). The organic layer was isolated, dried ($MgSO_4$) and the solvent removed *in vacuo*. The crude residue was purified by flash column chromatography on silica gel (CH_2Cl_2), followed by repeated recrystallization (hexane) of the desired fraction to yield the required 4-(4-*n*-alkoxyphenylazo)phenols (**4a**–**j**), 4-(4-*n*-alkoxyphenylazo)-fluorophenols (e.g. **5a**–**j**, **6a**–**j**) and 4-(4-*n*-alkoxyphenylazo)difluorophenols (e.g. **7a**–**j**, **8a**–**j**, **9a**–**j**).

4-(4-*n*-Alkoxyphenylazo)phenols (4a–j). The following spectroscopic data for 4-(4-*n*-heptyloxyphenylazo)phenol (**4g**) is representative for the remaining members of the non-fluorinated phenylazophenols (**4a**–**j**): ν_{max} (KBr)/cm^{-1}: 3320sb (O–H_{st}), 3039w (Ar–H_{st}), 2953, 2934, 2857w (C–H_{st}), 1597, 1498s (C=C_{st}) 1472s (C–H_{st}), 1244, 1105m (C–O_{st}), 842s (C–H_{def}, 2 adjacent H); δ_H (270 MHz: $CDCl_3$; Me_4Si) 0.89 (3H, t, CH_3), 1.32 (8H, m, CH_2), 1.81 (2H, quint, $\underline{CH_2}$–CH_2–O), 4.02 (2H, t, CH_2–O), 5.4 (1H, s, –OH,), 6.95 (2H, d, ArH), 7.0 (2H, d, ArH), 7.8 (2H,d, ArH), 7.83 (2H, d, ArH); δ_C (67.9 MHz: $CDCl_3$; Me_4Si) 14.08, 22.61, 25.98, 29.06, 29.2 ($\underline{CH_2}$–CH_2–O), 31.8 (CH_2), 68.35 (CH_2–O), 114.7 (ArC), 115.76 (ArC), 124.35 (ArC), 124.53 (ArC), 146.75 (ArC_Q), 158.86 (Ar_Q–OH), 161.27 (Ar_Q–OR). CHN found: C, 72.93%; H, 7.66%; N, 8.94%. Requires: C, 73.05%; H, 7.74%; N, 8.97%. Melting point 104.5°C.

3-Fluoro-4-(4-*n*-alkoxyphenylazo)phenols (5a–j). The following spectroscopic data for 3-fluoro-4-(4-*n*-heptyloxyphenylazo)phenol (**5g**) is representative for the remaining members of this fluorinated series: ν_{max} (KBr)/cm^{-1}: 3404 s.br (O–H_{str}), 3074w (Ar–H_{str}), 2998, 2949, 2848w (C–H_{str}), 1601, 1497s (C=C_{str}) 1266, 1113m (C–O_{str}), 837s (C–H_{def}, 2 adjacent H); δ_H

(270 MHz; $CDCl_3$; Me_4Si) 0.92 (3H, t, CH_3), 1.41 (8H, m, $CH_3\underline{CH_2}CH_2$–), 1.81 (2H, quint, $\underline{CH_2}$–CH_2–O), 4.01 (2H, t, –$CH_2\underline{CH_2}$OAr), 5.7 (1H, s, –OH), 6.4 (1H, d, ArH), 6.66 (1H, d, ArH), 6.98 (2H,d, ArH), 7.68 (1H, t, ArH), 7.88 (2H, d, ArH); δ_C (67.9 MHz: $CDCl_3$; Me_4Si) 14.07 (CH_3), 22.65, 26.0, 29.18, 29.2, 31.8 (CH_2), 68.41 (CH_2–O), 103.9 (ArC, $^2J_{CF}$=22.8 Hz), 111.7 (ArC, $^4J_{CF}$=3 Hz), 114.72 (ArC), 119 (ArC), 124.79 (ArC), 135.3 (ArC_Q, $^2J_{CF}$=6.7 Hz), 147.12 (ArC_Q), 158.86 (ArC_Q–OH, $^3J_{CF}$=11.41 Hz), 158.99+162.78 (Ar–F, $^1J_{CF}$=257 Hz), 161.62 (ArC_Q–OR). CHN expected: C, 69.07%; H, 7.02%; N, 8.48%. CHN found: C, 69.14%; H, 7.08%; N, 8.48%. Melting point 98°C.

2-Fluoro-4-(4-*n*-alkoxyphenylazo)phenols (6a–j). The following spectroscopic data for 2-fluoro-4-(4-*n*-heptyloxyphenylazo)phenol (**6g**) is representative for the remaining members of this fluorinated series: ν_{max} (KBr)/cm^{-1}: 3404s,br (O–H_{str}), 3074w (Ar–H_{str}), 2998, 2949, 2848w (C–H_{str}), 1601, 1497s (C=C_{str}) 1266, 1113m (C–O_{str}), 837s (C–H_{def}, 2 adjacent H); δ_H (270 MHz: $CDCl_3$; Me_4Si) 0.92 (3H, t, CH_3), 1.41 (2H, sext, $CH_3\underline{CH_2}CH_2$–), 1.81 (2H, quint, $\underline{CH_2}$–CH_2–O), 4.01 (2H, t, –$CH_2\underline{CH_2}$OAr), 5.53 (1H, s, –OH), 6.96 (2H, d, ArH), 7.08 (1H, t, ArH), 7.63 (1H, d, ArH), 7.67 (1H, d, ArH), 7.85 (2H, d, ArH); δ_C (67.9 MHz: $CDCl_3$; Me_4Si) 14.07 (CH_3), 22.65, 26.0, 29.18, 29.2, 31.8 (CH_2), 68.41 (CH_2–O), 107.7 (ArC $^2J_{CF}$=18.68 Hz), 114.72 (ArC), 117.03 (ArC, $^3J_{CF}$=2.07 Hz), 122.1 (ArC $^4J_{CF}$=3.11 Hz), 124.6 (ArC), 145.7 (ArC_Q–OH, $^2J_{CF}$=14.53 Hz), 146.5 (ArC_Q), 146.8 (ArC_Q, $^3J_{CF}$=5.19 Hz), 149.61+153.14 (Ar–F, $^1J_{CF}$=240 Hz), 161.55 (ArC_Q–OH). Melting point 92°C.

2,3-Difluoro-4-(4-*n*-alkoxyphenylazo)phenols (7a–j). The following spectroscopic data for 2,3-difluoro-4-(4-*n*-heptyloxyphenylazo)phenol (**7g**) is representative for the remaining members of this fluorinated series: ν_{max} (KBr)/cm^{-1}: 3392s,br (O–H_{str}), 3070w (Ar–H_{str}), 2992, 2949, 2846w (C–H_{str}), 1600, 1491s (C=C_{str}) 1244, 1105m (C–O_{str}), 830s (C–H_{def}, 2 adjacent H); δ_H (270 MHz; $CDCl_3$; Me_4Si) 0.87 (3H, t, CH_3), 1.29 (8H, m, CH_2) 1.79 (2H, quint, $\underline{CH_2}$–CH_2–O), 4.01 (2H, t, $CH_2\underline{CH_2}$OAr), 6.0 (1H, s, OH), 6.79 (1H, t, ArH), 6.96 (2H, d, ArH), 7.49 (1H, t, ArH), 7.87 (2H, d, ArH); δ_C (67.9 MHz: $CDCl_3$; Me_4Si) 14.06 (CH_3) 22.63, 26, 29.16, 29.2, 31.74 (CH_2), 68.44 (CH_2–O), 111.8 (ArC_Q $^4J_{CF}$=3.11 Hz), 112.15 (ArC_Q $^4J_{CF}$=3.11 Hz), 114.75 (ArC), 124.8 (ArC), 135.67 (ArC_Q, $^2J_{CF}$=5.2 Hz), 138.56–142.3 (ArC_Q, $^1J_{CF}$=240 Hz, $^2J_{CF}$=13.5 Hz), 146.74 (ArC_Q), 146.9 (ArC_Q–OH), 147–150.89 (Ar–F, $^1J_{CF}$=261 Hz, $^2J_{CF}$=11.4 Hz), 162.5 (ArC_Q–OR). CHN expected: C, 65.5%; H, 6.36%; N, 8.04%. CHN found: C, 65.7%; H, 6.42%; N, 7.9%. Melting point 101°C.

2,6-Difluoro-4-(4-*n*-alkoxyphenylazo)phenols (8a–j). The following spectroscopic data for 2,6-difluoro-4-(4-*n*-heptyloxyphenylazo)phenol (**8g**) is representative for the remaining members of this fluorinated series: ν_{max} (KBr)/cm^{-1}: 3320s,b (O–H_{st}), 3039w (Ar–H_{st}), 2953, 2934, 2857w (C–H_{st}), 1597, 1498s (C=C_{st}) 1472s (C–H_{st}), 1244, 1105m (C–O_{st}), 842s (C–H_{def}, 2 adjacent H); δ_H (270 MHz: $CDCl_3$; Me_4Si) 0.88 (3H, t, CH_3), 1.29 (8H, m, CH_2) 1.82 (2H, quint, $\underline{CH_2}$–CH_2–O) 4.03 (2H, t, –$CH_2\underline{CH_2}$OAr), 5.47 (1H, s, –OH), 6.96 (2H, d, ArH, J=8.8 Hz) 7.52 (2H, d, ArH) 7.84 (2H, d, ArH, J=8.8 Hz); δ_C (67.9 MHz: $CDCl_3$; Me_4Si) 14.07, 22.65, 31.8 ($\underline{CH_2}$–CH_2–O), 68.41 (CH_2–O), 106.4 (ArC $^2J_{CF}$=23.87 Hz) 114.88 (ArC) 124.96 (ArC) 134.62 (ArC_Q, $^2J_{CF}$=21.5 Hz) 145.22 (ArC_Q, $^3J_{CF}$=7.26 Hz) 146.37 (ArC_Q) 149.97+153.6 (Ar–F, $^1J_{CF}$=240 Hz, $^3J_{CF}$=5.71 Hz) 162.51 (ArC_Q–OR). CHN expected: C, 65.5%; H, 6.36%; N, 8.04%. CHN found: C, 65.61%; H, 6.4%; N, 7.94%. Melting point 96°C.

3,5-Difluoro-4-(4-*n*-alkoxyphenylazo)phenols (9a–j). The following spectroscopic data for 3,5-difluoro-4-(4-*n*-heptyloxyphenylazo)phenol (**9g**) is representative for the remaining members of this fluorinated series: ν_{max} (KBr)/cm^{-1}: 3534s,b (O–H_{str}), 3074w (Ar–H_{str}), 2953, 2934, 2857 (C–H_{st}), 1597, 1498s (C=C_{st}), 1472s (C–H_{st}), 1244, 1105s/m (C–O_{str}), 842s (C–H_{def}, 2 adjacent H); δ_H (270 MHz: $CDCl_3$; Me_4Si) 0.88 (3H, t, CH_3), 1.33 (8H, m, CH_2) 1.82 (2H, quint, $\underline{CH_2}$–CH_2–O) 4.02 (2H, t, –$CH_2\underline{CH_2}$OAr), 6.29 (1H, s, –OH), 6.48 (2H, d, ArH), 6.97 (2H, d, ArH), 7.89 (2H, d, ArH); δ_C (67.9 MHz: $CDCl_3$; Me_4Si) 14.09 (1, CH_3), 22.64, 25.98, 29.14, 29.21, 31.8 (CH_2), 68.41 (CH_2–O), 100.25 (ArC $^2J_{CF}$=24.9 Hz), 114.7 (ArC and ArC_Q), 124.57 (ArC), 147.6 (ArC_Q), 155.84–158.35 (Ar–F, $^1J_{CF}$=253 Hz, $^3J_{CF}$=8.62 Hz), 157.26 (ArC_Q–OH, $^3J_{CF}$=14.37 Hz), 161.99 (8, ArC_Q–OH). CHN expected: C, 66.28%; H, 6.67%; N, 7.73%. CHN found: C, 66.18%; H, 6.77%; N, 7.68%. Melting point 99°C.

2.2.2. General method for esterification (series I–XIII). A mixture of the appropriate acid (either 3-(2-thienyl)acrylic acid or 3-(3-thienyl)acrylic acid or *trans*-cinnamic acid; 2.22 mmol), the appropriate 'azophenol' (**4**–**9**) (2.02 mmol), dicyclohexylcarbodiimide (2.22 mmol), dimethylaminopyridine (0.2 mmol) and dry CH_2Cl_2 (20 ml) was stirred at room temperature overnight. The ensuing white precipitate was isolated by Büchner filtration and discarded, whilst the filtrate was evaporated to dryness *in vacuo*. The resultant crude residue was purified by column chromatography on silica gel eluting with dichloromethane, followed by repeated recrystallization from toluene until constant transition

temperatures were achieved. The transition temperatures for the members of series **I**–**XIII** are listed in tables 1–13, respectively.

3-(Thiophen-2-yl)-acrylic acid 4-(4-*n*-alkoxyphenylazo)phenyl esters (series I; 10a–j). The following spectroscopic data for 3-thiophen-2-yl-acrylic acid 4-(4-*n*-heptyloxyphenylazo)phenyl ester is representative for the remaining members of series **I**: ν_{max} (KBr)/cm^{-1}: 3092.5w (Ar–H_{str}), 2937, 2855w (C–H_{str}), 1730s (C=O_{str}), 1630s (alkene C=C_{str}), 1602, 1498s (C=C_{str}), 1256, 1112s (C–O_{str}), 843s (C–H_{def}, 2 adjacent H); δ_H (270 MHz: $CDCl_3$; Me_4Si) 0.9 (3H, t, CH_3), 1.32 (8H, m, –$(CH_2)_4$–), 1.84 (2H, quint, $\underline{CH_2}$–CH_2–O), 4.03 (2H, t, $\underline{CH_2}$–O), 6.43 (1H, d, $\underline{CH}$=CH–O, J=16 Hz), 7.0 (2H,d, ArH), 7.1 (1H, m, $ArH_{[Thio]}$, J=4.1 Hz), 7.31 (2H, d ArH), 7.32 (1H, d, $ArH_{[Thio]}$, J=3.2 Hz), 7.43 (1H, d, $ArH_{[Thio]}$, J=5.1 Hz), 7.9 (2H, d, ArH), 7.91(2H, d, ArH), 7.92 (1H, d, CH=$\underline{CH}$–O, J=16 Hz); δ_C (67.9 MHz: $CDCl_3$; Me_4Si) 14.08, 22.61, 25.99, 29.06, 29.21 ($\underline{CH_2}$–CH_2–O), 31.78 (CH_2), 68.39 (CH_2–O), 114.67 (Ar–C), 115.62 ($\underline{CH}$=CH–O), 122.14 (ArC), 123.69 (ArC), 124.76 (ArC), 128.29 ($ArC_{[Thio]}$), 129.31 ($ArC_{[Thio]}$), 131 ($ArC_{[Thio]}$), 139.23 (CH=$\underline{CH}$–O), 139.29 ($ArC_{Q[Thio]}$), 146.8 (ArC_Q), 150.38 (ArC_Q), 152.29 (ArC_Q), 161.75 (ArC_Q–O), 164.96 (CO_2). CHN expected: C, 69.62%; H, 6.29%; N, 6.24%. CHN found: C, 69.64%; H, 6.24%; N, 6.24%. HRMS (ESCI) 449.1893 (M+H).

3-(Thiophen-2-yl)-acrylic acid 4-(4-*n*-alkoxyphenylazo)-2-fluorophenyl esters (series VI; 14a–d). The following spectroscopic data for 3-thiophen-2-yl-acrylic acid 4-(4-*n*-butyloxyphenylazo)-2-fluorophenyl ester is representative for the remaining members of series **VI**: ν_{max} (KBr)/cm^{-1}: 3092w (Ar–H_{str}), 2920, 2851w (C–H_{str}), 1735s (C=O_{str}), 1620s (alkene C=C_{str}), 1601, 1498s (C=C_{str}), 1255, 1121s (C–O_{str}), 838s (C–H_{def}, 2 adjacent H); δ_H (270 MHz: $CDCl_3$; Me_4Si) 0.92 (3H, t, CH_3), 1.41 (2H, sext, $CH_3\underline{CH_2}CH_2$–), 1.81 (2H, quint, $\underline{CH_2}$–CH_2–O), 4.01 (2H, t, –$CH_2\underline{CH_2}$OAr), 6.4 (1H, d, $\underline{CH}$=CH–O, J=15 Hz), 7.0 (2H, d, ArH), 7.09 (3H, m, ArH and $ArH_{[Thio]}$), 7.34 (1H, d, $ArH_{[Thio]}$ J=3.97 Hz), 7.45 (1H, d, $ArH_{[Thio]}$, J=6.03 Hz), 7.8 (1H, t, ArH), 7.93 (2H, d, ArH), 8.0 (1H, d, CH=$\underline{CH}$–O, J=15 Hz); δ_C (67.9 MHz: $CDCl_3$; Me_4Si) 14.07, 22.65, 31.8 ($\underline{CH_2}$–CH_2–O), 68.41 (CH_2–O), 110.7 (ArC, $^2J_{CF}$=22.8 Hz), 114.76 (ArC), 115.2 ($\underline{CH_2}$=CH_2–O), 117.65 (ArC,

Table 1. Transition temperatures (°C) for a homologous series of 3-thiophen-2-yl acrylic acid 4-(4-*n*-alkoxyphenylazo)phenyl esters (series **I**). Enthalpy values (kJ mol^{-1}) are shown in italics.

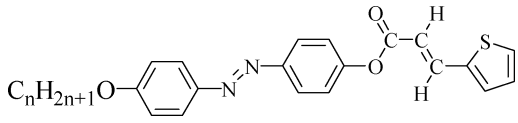

n-alkyl	C–C	C–N	N–I	I–N	N–C	$T_{N-I} - T_{C-N}$
CH_3	147.8	161.7	235.7	233.4	105.6	74
	1.1	*20.1*	*1.34*	*1.34*	*28.2*	
C_2H_5	—	178.2	235.1	233	124	56.9
		38.1	*1.69*	*1.94*	*26.6*	
C_3H_7	—	150.3	216.3	215.2	111	66
		57.8	*1.6*	*1.4*	*31*	
C_4H_9	—	159.2	215.7	214.3	130.1	56.5
		41.4	*2*	*2*	*36.3*	
C_5H_{11}	—	133.5	201.4	200.5	108.2	67.9
		34.5	*1.6*	*1.7*	*30.2*	
C_6H_{13}	—	136	197.8	195.8	109.9	61.8
		36.5	*1.8*	*1.8*	*32.9*	
C_7H_{15}	115.8	124.3	187.1	186.2	96.8	62.8
	5.02	*44.6*	*1.6*	*1.7*	*30.3*	
C_8H_{17}	—	118.7	183.7	182.4	98.9	65
		34	*1.7*	*1.6*	*30.1*	
C_9H_{19}	—	130.3	176.1	175.2	113.5	45.8
		56.2	*1.5*	*1.45*	*45.5*	
$C_{10}H_{21}$	—	112.3	172.4	171.3	89.6	60.1
		41	*1.7*	*1.6*	*34*	
Average			202.1			61.7

Table 2. Transition temperatures (°C) for a homologous series 3-thiophen-3-yl-acrylic acid 4-(4-*n*-alkoxyphenylazo)phenyl esters (series **II**). Enthalpy values (kJ mol^{-1}) are shown in italics.

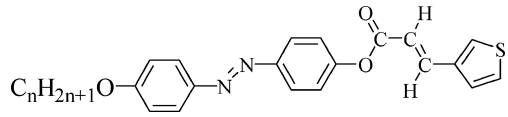

n-alkyl	C–C	C–N	N–I	I–N	N–C	$T_{N-I} - T_{C-N}$
CH_3	—	164.5	234.9	233.8	119.3	70.4
		51.9	*1.8*	*1.8*	*48.2*	
C_2H_5	—	161.1	243.2	240.6	125	82.1
		37.1	*2.8*	*3.1*	—[a]	
C_3H_7	—	156.2	226	224.7	120.1	69.8
		39.1	*1.9*	*1.9*	*27.7*	
C_4H_9	105.8[b]	154.4	224.6	222.9	122.5	70.2
	9.7	*42.3*	*2.6*	*3.0*	*33.3*	
C_5H_{11}	—	136.4	210	208.7	109.3	73.6
		36.2	*2.3*	*2.4*	*21.6*	
C_6H_{13}	93.5[b]	134	204	201.5	105.3	70
	10.1	*35.3*	*2.5*	*2.5*	—[a]	
C_7H_{15}	121.6[b]	133.5	195.9	194.5	106.6	62.4
	24.7	*35.2*	*1.8*	*2.1*	*28.6*	
C_8H_{17}	—	126.6	191	190	96.3	64.4
		38.1	*2.0*	*2.1*	*22.5*	
C_9H_{19}	—	137.7	183.4	182.1	115.7	45.7
		62.9	*1.6*	*1.8*	*31.4*	
$C_{10}H_{21}$	110.1[b]	123.3	180.7	179.2	97.6	57.4
	48.6	*20.2*	*1.8*	*1.8*	*33.8*	
Average			209.4			66.6

[a]Unresolvable: two large overlapping peaks. [b]Detected by differential scanning calorimetry on first heat.

$^4J_{CF}$=3.11 Hz), 118.22 (ArC), 125.13 (ArC), 128.34 ($ArC_{[Thio]}$), 129.53 ($ArC_{[Thio]}$), 131.9 ($ArC_{[Thio]}$), 138.5 (ArC_Q, $^2J_{CF}$=7.27 Hz), 139.14 ($ArC_{Q[Thio]}$), 139.68 (CH=<u>CH</u>–O), 147.1 (ArC_Q), 152.9 (ArC_Q, $^3J_{CF}$=11.41 Hz), 157.87+161.68 (Ar–F, $^1J_{CF}$=258 Hz), 162.14 (ArC_Q–O), 164.49 (CO_2). $C_{23}H_{21}FN_2O_3S$ expected: C, 65.08%; H, 4.99%; F, 4.48%; N, 6.60%; O, 11.31%; S, 7.55%. CHN found: C, 64.99%; H, 4.95%; N, 6.61%. HRMS (ESCI) 425.1335 (M+H).

3-(Thiophen-2-yl)-acrylic acid 4-(4-*n*-alkoxyphenylazo)-3-fluorophenyl esters (series IV; 13a–d). The following spectroscopic data for 3-thiophen-2-yl-acrylic acid 3-fluoro-4-(4-*n*-butyloxyphenylazo)-3-fluorophenyl ester is representative for the remaining members of series **IV**: ν_{max} (KBr)/cm^{-1}: 3061w (Ar–H_{str}), 2927, 2858w (C–H_{str}), 1735s (C=O_{str}), 1623s (alkene C=C_{str}), 1596, 1493s (C=C_{str}), 1268–1122s (C–O_{str}), 878s (C–H_{def}, 2 adjacent H); δ_H (270 MHz: $CDCl_3$; Me_4Si) 0.92 (3H, t, CH_3), 1.41 (2H, sext, CH_3<u>CH_2</u>CH_2–), 1.81 (2H, quint, <u>CH_2</u>–CH_2–O), 4.01 (2H, t, –CH_2<u>CH_2</u>OAr), 6.46(1H, d, <u>CH_2</u>=CH_2–O, J=16 Hz), 7.0 (2H, d, ArH), 7.08 (1H, t, $ArH_{[Thio]}$, J=3.7 Hz), 7.36 (2H, m, $ArH_{[Thio]}$ and Ar–H), 7.45 (1H, d, Ar–H), 7.72 (2H, m, ArH and Ar–H), 7.89 (2H, d, ArH), 7.9 (1H, d, CH=<u>CH</u>–O, J=16 Hz); δ_C (67.9 MHz: $CDCl_3$; Me_4Si) 14.07, 22.65, 31.8 (<u>CH_2</u>–CH_2–O), 68.41 (CH_2–O), 108.9 (ArC, $^2J_{CF}$=19.72 Hz), 114.64 (ArC), 114.77 (<u>CH_2</u>=CH_2–O), 120.64 (ArC, $^4J_{CF}$=3.11 Hz), 123.86 (ArC), 125.01 (Ar–C), 125.18 ($ArC_{[Thio]}$), 127.28 ($ArC_{[Thio]}$), 129.38 ($ArC_{[Thio]}$), 139.15 ($ArC_{Q[Thio]}$), 139.6 (ArC_Q, $^2J_{CF}$=13.49 Hz), 139.89 (CH=<u>CH</u>–O, J=15.56 Hz), 146.51 (ArC_Q), 151.3 (ArC_Q, $^3J_{CF}$=5.2 Hz), 152.74+156.44 (Ar–F, $^1J_{CF}$=250 Hz), 162.14 (ArC_Q–O), 164.37 (CO_2). $C_{23}H_{21}FN_2O_3S$ expected: C, 65.08%; H, 4.99%; F, 4.48%; N, 6.60%; O, 11.31%; S, 7.55%. CHN found: C, 65.08%; H, 4.94%; N, 6.66%. HRMS (ESCI) 425.1326 (M+H).

3-(Thiophen-2-yl)-acrylic acid 4-(4-*n*-alkoxyphenylazo)-2,3-difluorophenyl esters (series VIII; 15a–d). The following spectroscopic data for 3-thiophen-2-yl-acrylic acid 4-(4-*n*-butyloxyphenylazo)-2,3-difluorophenyl ester is representative for the remaining members of series **VIII**: ν_{max} (KBr)/cm^{-1}: 3071w (Ar–H_{str}), 2928, 2859w (C–H_{str}), 1739s (C=O_{str}), 1621s (alkene C=C_{str}), 1598, 1496s (C=C_{str}), 1259, 1115s (C–O_{str}), 853s (C–H_{def}, 2 adjacent H); δ_H (270 MHz: $CDCl_3$; Me_4Si) 0.92 (3H, t,

Table 3. Transition temperatures (°C) for a homologous series of acid 4-(4-*n*-alkoxyphenylazo)phenyl cinnamates (series **III**). Enthalpy values (kJ mol^{-1}) are shown in italics.

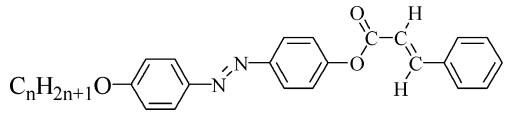

n-alkyl	C–C	C–N	N–I	I–N	N–C	$T_{N-I} - T_{C-N}$
CH_3	—	146.5	242.4	240.6	105.8	95.9
		28.7	*1.3*	*1.3*	*23*	
C_2H_5	—	161.7	246.5	244.2	130.2	84.8
		34.4	*1.8*	*1.9*	*31.1*	
C_3H_7	93	140.5	225.7	223.8	109.2	85.2
	9.2	*33.4*	*1.6*	*1.6*	*29.1*	
C_4H_9	—	139.5	223.5	221.7	105.1	84
		34.6	*1.7*	*1.7*	*30.2*	
C_5H_{11}	98.3	121.8	209	208	95.2	87.2
	3.9	*30*	*1.5*	*1.5*	*27*	
C_6H_{13}	—	118.9	204.9	204	94.5	85.7
		35.7	*1.5*	*1.6*	*31.5*	
C_7H_{15}	—	117.3	195	193.6	94.7	77.7
		36.9	*1.6*	*1.5*	*32.5*	
C_8H_{17}	—	118.3	190.8	189.7	93.4	72.5
		41.9	*1.5*	*1.6*	*34*	
C_9H_{19}	—	117.2	194	192.6	92.1	76.8
		32.4	*1.4*	*1.4*	*37.8*	
$C_{10}H_{21}$	—	116.3	189	188	91.4	72.7
		36.6	*1.7*	*1.6*	*33.3*	
Average			212.1			82.3

CH_3), 1.41 (2H, sext, $CH_3\underline{CH_2}CH_2$–), 1.81 (2H, quint, $\underline{CH_2}$–CH_2–O), 4.01 (2H, t, –$CH_2\underline{CH_2}$OAr), 6.42 (1H, d, $\underline{CH_2}$=CH_2–O J=16 Hz), 7.0 (2H, d, ArH), 7.09 (2H, m, ArH and $ArH_{[Thio]}$), 7.35 (1H, d, $ArH_{[Thio]}$, J=3.46 Hz), 7.45 (1H, d, $ArH_{[Thio]}$, J=4.95Hz), 7.55 (1H, t, ArH), 7.93 (2H, d, ArH), 8.1 (1H, d, CH=$\underline{CH}$=O, J=16 Hz); δ_C (67.9 MHz: $CDCl_3$; Me_4Si) 14.07, 22.65, 31.8 ($\underline{CH_2}$–CH_2–O), 68.41 (CH_2–O), 111.7 (ArC, $^3J_{CF}$=4.16 Hz),

Table 4. Transition temperatures (°C) for a homologous series of 3-thiophen-2-yl-acrylic acid 4-(4-*n*-alkoxyphenylazo)-3-fluorophenyl esters (series **IV**). Enthalpy values (kJ mol^{-1}) are shown in italics.

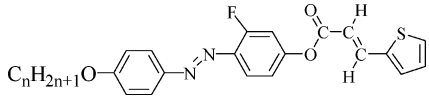

n-alkyl	C–C	C–N	N–I	I–N	N–C	$T_{N-I} - T_{C-N}$
CH_3	140.3	169.4	215.4	214.5	119.8	46
	15.3	*30.3*	*1.6*	*1.5*	*41.3*	
C_2H_5	—	147	216	214.4	130.3	69
		31.6	*1.7*	*1.6*	*43*	
C_3H_7	—	134.6	197.9	195.5	82.3	63.3
		33.5	*1.5*	*1.6*	*33.9*	
C_4H_9	—	129.4	196.5	195.9	113	67.1
		72.2	*3.5*	*3.9*	*78.4*	
Average			206.5			61.4

Table 5. Transition temperatures (°C) for a homologous series of 3-thiophen-2-yl-acrylic acid 4-(4-*n*-alkoxyphenylazo)-2-fluorophenyl esters (series **VI**). Enthalpy values (kJ mol^{-1}) are shown in italics.

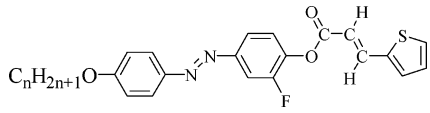

n-alkyl	C–C	C–N	N–I	I–N	N–C	$T_{N-I} - T_{C-N}$
CH_3	—	177.4	215.9	214.5	112.9	38.5
		36.7	*1.5*	*1.5*	*31.8*	
C_2H_5	—	181.5	220	218.6	133.6	38.5
		44	*2.1*	*2.1*	*41.7*	
C_3H_7	—	160.3	200	198.4	117.4	39.7
		39.3	*1.8*	*1.8*	*35.6*	
C_4H_9	—	143.1	199	196.5	117.4	55.9
		38.5	*2.1*	*2*	*31.3*	
Average			208.7			43.2

114 (CH=CH–O), 114.8 (ArC), 118.03 (ArC, $^3J_{CF}$=4.16 Hz), 125.4 (ArC), 128.34 ($ArC_{[Thio]}$), 129.76 ($ArC_{[Thio]}$), 132.17 ($ArC_{[Thio]}$), 139 ($ArC_{Q[Thio]}$), 139.7 (ArC_Q, $^2J_{CF}$=5.2 Hz), 140.3 (CH=CH–O), 140.5 (ArC_Q, $^2J_{CF}$=14.5 Hz), 140.67–145.97 (Ar–F, $^1J_{CF}$=252 Hz, $^3J_{CF}$=12.46 Hz), 146.92 (ArC_Q), 147+150.87 (Ar–F, $^1J_{CF}$=257 Hz, $^3J_{CF}$=11.42 Hz), 162.47 (ArC_Q–O), 163.57 (CO_2). $C_{23}H_{20}F_2N_2O_3S$ expected: C, 62.43%; H, 4.56%; F, 8.59%; N, 6.33%; O, 10.85%; S, 7.25%. CHN found: C, 62.39%; H, 4.49%; N, 6.35%. HRMS (ESCI) 443.1232 (M+H).

3-(Thiophen-2-yl)-acrylic acid 4-(4-*n*-alkoxyphenylazo)-3,5-difluorophenyl esters (series XII; 17a–d). The following spectroscopic data for 3-thiophen-2-yl-acrylic acid 4-(4-*n*-butyloxyphenylazo)-3,5-difluorophenyl ester is representative for the remaining members of series **XII**: ν_{max} (KBr)/cm^{-1}: 3123w (Ar–H_{str}), 2950, 2853w (C–H_{str}), 1734s (C=O_{str}), 1616s (alkene C=C_{str}), 1597, 1502s (C=C_{str}), 1255, 1122s (C–O_{str}), 834s (C–H_{def}, 2 adjacent H); δ_H (270 MHz: $CDCl_3$; Me_4Si) 0.92 (3H, t, CH_3), 1.41 (2H, sext, $CH_3CH_2CH_2$–), 1.81 (2H, quint, CH_2–CH_2–O), 4.01 (2H, t, –CH_2CH_2OAr), 6.52 (1H, d, CH=CH–O, J=16 Hz), 7.0 (2H, d, ArH), 7.05 (2H, d, ArH), 7.1 (1H, t, $ArH_{[Thio]}$, J=5.64 Hz), 7.34 (2H, d, $ArH_{[Thio]}$, J=3.5 Hz), 7.47 (1H, d, $ArH_{[Thio]}$, J=5 Hz), 7.49 (1H, d, $ArH_{[Thio]}$), 7.88 (2H, d, ArH), 7.89 (1H, d, CH=CH–O, J=16 Hz); δ_C (67.9 MHz: $CDCl_3$; Me_4Si) 14.07, 22.65, 31.8 (CH_2–CH_2–O), 68.41 (CH_2–O),

Table 6. Transition temperatures (°C) for a homologous series of 3-thiophen-2-yl-acrylic acid 4-(4-*n*-alkoxyphenylazo)-2,3-difluorophenyl esters (series **VIII**). Enthalpy values (kJ mol^{-1}) are shown in italics.

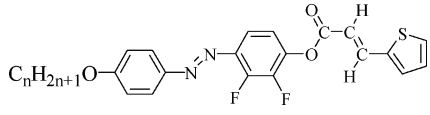

n-alkyl	C–C	C–N	N–I	I–N	N–C	$T_{N-I} - T_{C-N}$
CH_3	—	147.1	215.8	213.5	97.2	68.7
		30.6	*1.2*	*1.4*	*27.2*	
C_2H_5	—	158	221.7	219.6	114.5	63.7
		29.9	*1.2*	*1.3*	*26.1*	
C_3H_7	—	144.9	201.1	200.5	133	56.2
		35.6	*1.7*	*1.6*	*31.1*	
C_4H_9	—	140.1	199.7	198.1	86.5	59.6
		34.6	*2*	*1.8*	*38.5*	
Average			209.6			62.1

Table 7. Transition temperatures (°C) for a homologous series of 3-thiophen-2-yl-acrylic acid 4-(4-*n*-alkoxyphenylazo)-2,6-difluorophenyl esters (series **X**). Enthalpy values (kJ mol^{-1}) are shown in italics.

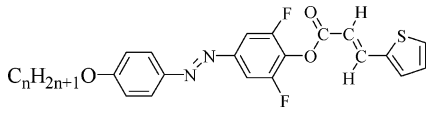

n-alkyl	C–C	C–N	N–I	I–N	N–C	$T_{N-I} - T_{C-N}$
CH_3	—	157.5	193.5	191	115	36
		*	*	*	*	
C_2H_5	—	181.3	204.4	202.6	155.1	23.1
		36.4	*2.5*	*2.5*	*35.3*	
C_3H_7	—	159.6	183.7	182.9	143.9	24.1
		34.2	*2.3*	*2.2*	*33.5*	
C_4H_9	146.8	150.1	181.9	181	123	31.8
	8.2	*28.1*	*2.9*	*2.5*	*29.3*	
Average			190.9			28.8

*Enthalpy value not available.

106.47 (ArC $^2J_{CF}$=23.87 Hz), 113.75 (<u>CH</u>$_2$=CH$_2$–O), 114.83 (ArC), 124.06 (ArC_Q), 125.3 (ArC), 128.34 (Ar$C_{[Thio]}$), 129.8 (Ar$C_{[Thio]}$), 132.2 (Ar$C_{[Thio]}$), 139.04 (Ar$C_{Q[Thio]}$), 140.53 (CH=<u>CH</u>–O), 146.26 (ArC_Q), 150.36 (ArC_Q, $^3J_{CF}$=7.27 Hz), 153.65+157.42 (Ar–F, $^1J_{CF}$=251.2 Hz, $^3J_{CF}$=5.2 Hz), 162.52 (ArC_Q–O), 163.07 (CO_2). $C_{23}H_{20}F_2N_2O_3S$ expected: C, 62.43%; H, 4.56%; F, 8.59%; N, 6.33%; O, 10.85%; S, 7.25%. CHN found: C, 62.33%; H, 4.45%; N, 6.26%. HRMS (ESCI) 443.1238 (M+H).

3-(Thiophen-2-yl)-acrylic acid 4-(4-*n*-alkoxyphenylazo)-2,6-difluorophenyl esters (series X; 16a–d). The following spectroscopic data for 3-thiophen-2-yl-acrylic acid 4-(4-*n*-butyloxyphenylazo)-2,6-difluorophenyl ester is representative for the remaining members of series **X**: ν_{max} (KBr)/cm^{-1}: 3092w (Ar–H$_{str}$), 2937, 2865w (C–H$_{str}$), 1730s (C=O$_{str}$), 1630s (alkene C=C$_{str}$), 1602, 1498s (C=C$_{str}$), 1256, 1125s (C–O$_{str}$), 842s (C–H$_{def}$, 2 adjacent H); δ_H (270 MHz: $CDCl_3$; Me_4Si) 0.92 (3H, t, CH_3), 1.41 (2H, sext, CH_3<u>CH_2</u>CH_2–), 1.81 (2H, quint, <u>CH_2</u>–CH_2–O), 4.01 (2H, t, –CH_2<u>CH_2</u>OAr), 6.38 (1H, d, <u>CH</u>=CH–O, J=16 Hz), 6.94 (2H, d, ArH), 6.97 (2H,d, ArH), 7.09 (1H, t, Ar$H_{[Thio]}$, J=5.64 Hz), 7.35 (1H, d, Ar$H_{[Thio]}$, J=4.7 Hz), 7.45 (1H, d, Ar$H_{[Thio]}$, J=4.7 Hz), 7.89 (2H, d, ArH, J=8.9 Hz), 7.97 (1H, d, CH=<u>CH</u>–O, J=16 Hz); δ_C (67.9 MHz: $CDCl_3$; Me_4Si) 14.07, 22.65,

Table 8. Transition temperatures (°C) for a homologous series of 3-thiophen-2-yl-acrylic acid 4-(4-*n*-alkoxyphenylazo)-3,5-difluorophenyl esters (series **XII**). Enthalpy values (kJ mol^{-1}) are shown in italics.

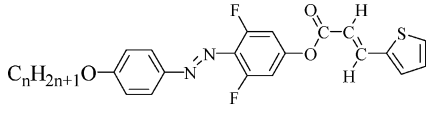

n-alkyl	C–C	C–N	N–I	I–N	N–C	$T_{N-I} - T_{C-N}$
CH_3	—	175.4	190	187	128	14.6
		38.2	*0.8*	*0.9*	*35.2*	
C_2H_5	—	149.4	205.1	203.5	140.2	55.7
		*	*	*	*	
C_3H_7	—	139.7	186.4	185.2	125	46.7
		41.3	*1.8*	*1.8*	*40*	
C_4H_9	—	140.6	186.9	185.2	127.8	46.3
		49.5	*2*	*2*	*47.7*	
Average			192.1			40.8

*Enthalpy value not available

Table 9. Transition temperatures (°C) for a homologous series of 3-thiophen-3-yl-acrylic acid 4-(4-*n*-alkoxyphenylazo)-3-fluorophenyl esters (series **V**). Enthalpy values (kJ mol^{-1}) are shown in italics.

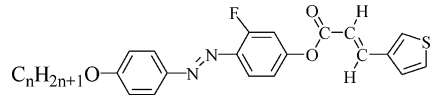

n-alkyl	C–C	C–N	N–I	I–N	N–C	$T_{N-I} - T_{C-N}$
CH_3	—	169.4	215.4	214.5	119.8	46
		43.6	*1.4*	*1.3*	*38.9*	
C_2H_5	—	150.6	223.6	220.9	128	73
		34.7	*2*	*2*	*33*	
C_3H_7	—	134.7	203.5	202.2	97.8	68.8
		33.3	*1.9*	*1.9*	*26.7*	
C_4H_9	—	119.1	201.2	200.1	96.2	82.1
		30.2	*2.1*	*2.2*	*31.7*	
Average			210.9			67.5

31.8 ($\underline{CH_2}$–CH_2–O), 68.41 (CH_2–O), 106.7 (ArC $^2J_{CF}$=28 Hz and $^3J_{CF}$=3.11 Hz), 114.7 (9, ArC and 17, $\underline{CH}$=CH–O), 125.04 (ArC and ArC_Q), 128.38 ($ArC_{[Thio]}$), 129.77 ($ArC_{[Thio]}$), 132.19 ($ArC_{[Thio]}$), 139 ($ArC_{Q[Thio]}$), 140.1 (CH=$\underline{CH}$–O), 147.6 (ArC_Q), 150.8 (ArC_Q, $^3J_{CF}$=13.5 Hz), 154+157.74 (13, Ar–F, $^1J_{CF}$=258 Hz, $^3J_{CF}$=7.26 Hz), 162.52 (ArC_Q–O), 164.1 (CO_2). $C_{23}H_{20}F_2N_2O_3S$ expected: C, 62.43%; H, 4.56%; F, 8.59%; N, 6.33%; O, 10.85%; S, 7.25%. CHN found: C, 62.35%; H, 4.47%; N, 6.28%. HRMS (ESCI) 443.1235 (M+H).

3-(Thiophen-3-yl)-acrylic acid 4-(4-*n*-alkoxyphenylazo)phenyl esters (series II; 12a–j). The following spectroscopic data for 3-thiophen-3-yl-acrylic acid 4-(4-*n*-heptyloxyphenylazo)phenyl ester is representative for the remaining members of series **II**: ν_{max} (KBr)/cm^{-1}: 3092.5w (Ar–H_{str}), 2937, 2855w (C–H_{str}), 1730s ($C{=}O_{str}$), 1630s (alkene $C{=}C_{str}$), 1602, 1498s ($C{=}C_{str}$), 1256, 1125s (C–O_{str}), 843s (C–H_{def}, 2 adjacent H); δ_H (270 MHz: $CDCl_3$; Me_4Si) 0.92 (3H, t, CH_3), 1.35 (8H, m, –$(CH_2)_4$–), 1.82 (2H, quint, $\underline{CH_2}$–CH_2–O), 4.04 (2H, t, CH_2–O), 6.46 (1H, d, $\underline{CH}$=CH–O, J=16 Hz), 7.0 (2H, d, ArH) 7.33 (2H, d ArH), 7.38 (2H, m, $ArH_{[Thio]}$), 7.59 (1H, t, $ArH_{[Thio]}$, H_F, J=2.1 Hz), 7.87 (1H, d, CH=$\underline{CH}$–O, J=15.8 Hz), 7.91 (2H, d, ArH), 7.3 (2H, d, ArH); δ_C (67.9 MHz: $CDCl_3$; Me_4Si) 14.06, 22.61, 25.7, 29.06, 29.15 (6, $\underline{CH_2}$–CH_2–O), 31.58 (CH_2), 68.33 (CH_2–O), 114.7 (ArC), 116.62 ($\underline{CH_2}$=CH_2–O), 122.17 (ArC), 123.69 (ArC), 124.77 (ArC), 125.15 ($ArC_{[Thio]}$), 127.26(20, $ArC_{[Thio]}$), 129.14 (22, Ar–$C_{[Thio]}$), 137.31 ($ArC_{Q[Thio]}$), 140.29 (CH=$\underline{CH}$–O), 146.76 (ArC_Q), 150.35 (ArC_Q), 152.27 (ArC_Q), 161.75 (ArC_Q–O), 164.36 (CO_2). $C_{26}H_{28}N_2O_3S$ expected: C, 69.62%; H, 6.29%; N, 6.24%; O, 10.70%; S, 7.15%. CHN found C, 69.62%; H, 6.29%; N, 6.24%. HRMS (ESCI) 449.1901 (M+H).

Table 10. Transition temperatures (°C) for a homologous series of 3-thiophen-3-yl-acrylic acid 4-(4-*n*-alkoxyphenylazo)-2-fluorophenyl esters (series **VII**). Enthalpy values (kJ mol^{-1}) are shown in italics.

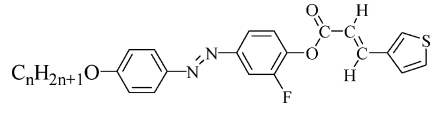

n-alkyl	C–C	C–N	N–I	I–N	N–C	$T_{N-I} - T_{C-N}$
CH_3	—	183	213.7	212.9	133.7	30.7
		38.5	*1.5*	*1.5*	*33.3*	
C_2H_5	—	195.4	221.8	219.8	152.4	26.4
		40.7	*2.3*	*2.1*	*37.5*	
C_3H_7	—	175.3	201.5	200	150.7	26.2
		40.7	*2.1*	*2*	*39.1*	
C_4H_9	—	152.8	200	199	120.5	47.2
		29.4	*1.1*	*1.9*	*28.6*	
Average			209.3			32.6

Table 11. Transition temperatures (°C) for a homologous series of 3-thiophen-3-yl-acrylic acid 4-(4-*n*-alkoxyphenylazo)-2,3-difluorophenyl esters (series **IX**). Enthalpy values (kJ mol^{-1}) are shown in italics.

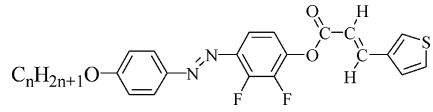

n-alkyl	C–C	C–N	N–I	I–N	N–C	$T_{N-I} - T_{C-N}$
CH_3	—	147.1	215.8	213.5	97.2	68.7
		34.5	*1.5*	*1.4*	*29.1*	
C_2H_5	—	157	224.5	222.2	127.7	67.5
		34.3	*2.3*	*2.3*	*32.8*	
C_3H_7	—	145	203.1	202	130.2	58.1
		29.7	*1.9*	*1.9*	*28.7*	
C_4H_9	—	126.1	200.2	199.2	80.5	74.1
		40.2	*2.3*	*2.3*	*30*	
Average			210.9			67.1

3-(Thiophen-3-yl)-acrylic acid 4-(4-*n*-alkoxyphenylazo)-2-fluorophenyl esters (series VII; 19a–d). The following spectroscopic data for 3-thiophen-3-yl-acrylic acid 2-fluoro-4-(4-*n*-butyloxyphenylazo)-phenyl ester is representative for the remaining members of series **VII**: ν_{max} (KBr)/cm^{-1}: 3092w (Ar–H_{str}), 2937, 2855w (C–H_{str}), 1730s (C=O_{str}), 1630s (alkene C=C_{str}), 1602, 1498s (C=C_{str}), 1256, 1125s (C–O_{str}), 843s (C–H_{def}, 2 adjacent H); δ_H (270 MHz: $CDCl_3$; Me_4Si) 0.92 (3H, t, CH_3), 1.41 (2H, sext, $CH_3\underline{CH_2}CH_2$–), 1.81 (2H, quint, $\underline{CH_2}$–CH_2–O), 4.01 (2H, t, –$CH_2\underline{CH_2}$OAr), 6.4 (1H, d, $\underline{CH}$=CH–O, J=16 Hz), 7.0 (2H, d, ArH), 7.04 (1H, m, ArH), 7.15 (1H, d, ArH), 7.36 (2H, m, $ArH_{[Thio]}$), 7.59 (1H, m, $ArH_{[Thio]}$), 7.8 (1H, d, ArH), 7.86 (1H, d, CH=$\underline{CH}$–O, J=16 Hz), 7.93 (2H, d, ArH); δ_C (67.9 MHz: $CDCl_3$; Me_4Si) 14.07, 22.65, 31.8 ($\underline{CH_2}$–CH_2–O), 68.41 (CH_2–O), 110.7 (ArC, $^2J_{CF}$=23.87 Hz), 114.72 (9, ArC), 116.17 (19, $\underline{CH}$=CH–O), 117.65 (Ar–H, $^4J_{CF}$=3.11 Hz), 118.16 (ArC), 125.12 (ArC and $ArC_{[Thio]}$), 127.34 ($ArC_{[Thio]}$), 129.34 $ArC_{[Thio]}$), 137.2 ($ArC_{Q[Thio]}$), 138.5 (ArC_Q, $^2J_{CF}$=7.27 Hz), 140.7 (CH=$\underline{CH}$–O), 147.06 (ArC_Q), 152.9 (ArC_Q, $^2J_{CF}$=11.41 Hz), 157.86+161.67 (Ar–F, $^1J_{CF}$=258 Hz), 162.11 (ArC_Q–O), 164.84 (CO_2). $C_{23}H_{21}FN_2O_3S$ Expected C, 65.08%; H, 4.99%; F, 4.48%; N, 6.60%; O, 11.31%; S, 7.55%. CHN found: C, 65.12%; H, 4.96%; N, 6.64%. HRMS (ESCI) 425.1323 (M+H).

3-(Thiophen-3-yl)-acrylic acid 4-(4-*n*-alkoxyphenylazo)-3-fluorophenyl esters (series V; 18a–d). The following spectroscopic data for 3-thiophen-3-yl-acrylic acid 4-(4-*n*-butyloxyphenylazo)-3-fluorophenyl ester is representative for the remaining members of series **V**: ν_{max} (KBr)/cm^{-1}: 3093w (C–H_{str}), 2919, 2857w (aliph C–H_{str}) 1736s (C=O_{str}), 1630s (alkene C=C_{str}), 1595,

Table 12. Transition temperatures (°C) for a homologous series of 3-thiophen-3-yl-acrylic acid 4-(4-*n*-alkoxyphenylazo)-2,6-difluorophenyl esters (series **XI**). Enthalpy values (kJ mol^{-1}) are shown in italics.

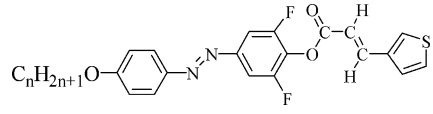

n-alkyl	C–C	C–N	N–I	I–N	N–C	$T_{N-I} - T_{C-N}$
CH_3	—	177.2	189.5	188.4	128.2	12.3
		32.1	*2*	*2*	*31.6*	
C_2H_5	—	198.2	199.8	199.4	189.4	1.6
		45	*	*2.8*	*42*	
C_3H_7	—	171.3	175.7	174.5	159.1	4.4
		32.4	*1**	2.2	*35.6*	
C_4H_9	—	156.1	175	174	130.9	18.9
		37.3	*2.6*	*2.7*	*34.5*	
Average			185.0			9.3

*Denotes more than one peak overlap.

Table 13. Transition temperatures (°C) for a homologous series of 3-thiophen-3-yl-acrylic acid 4-(4-*n*-alkoxyphenylazo)-3,5-difluorophenyl esters (series **XIII**). Enthalpy values (kJ mol^{-1}) are shown in italics.

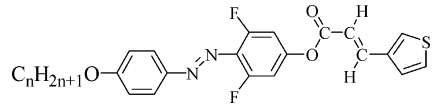

n-alkyl	C–C	C–N	N–I	I–N	N–C	$T_{N-I} - T_{C-N}$
CH_3	—	167.7	201.7	200.5	121.3	34
		41.3	*1.3*	*0.6*	*35*	
C_2H_5	—	148.3	210.1	208.3	133.3	61.8
C_3H_7	—	136.9	192.1	190.8	108.3	55.2
		34.5	*2*	*1.5*	*31.4*	
C_4H_9	—	129.4	191.8	190.6	111.5	62.4
		43.5	*2.6*	*2.6*	*32.4*	
Average			198.9			53.4

1493s (C=C_{str}), 1298, 1121s (C–O_{str}), 838s (C–H_{def}, 2 adjacent H); δ_H (270 MHz: $CDCl_3$; Me_4Si) 0.92 (3H, t, CH_3), 1.41 (2H, sext, $CH_3\underline{CH_2}CH_2$–), 1.81 (2H, quint, $\underline{CH_2}$–CH_2–O), 4.01 (2H, t, –$CH_2\underline{CH_2}$OAr), 6.46 (1H, d, $\underline{CH}$=CH–O, J=15.8 Hz), 7.0 (2H,d, ArH), 7.04 (3H, m, ArH and $ArH_{[Thio]}$), 7.36 (1H, t, $ArH_{[Thio]}$, J=1.92 Hz), 7.72 (2H, m, ArH), 7.87 (1H, d, CH=$\underline{CH}$–O, J=15.8 Hz), 7.9 (2H, d, ArH); δ_C (67.9 MHz: $CDCl_3$; Me_4Si) 14.07, 22.65, 31.8 ($\underline{CH_2}$–CH_2–O), 68.41 (CH_2–O), 108.9 (ArC, $^2J_{CF}$=19.72 Hz), 114.77 (ArC), 115.62 ($\underline{CH}$=CH–O, J=16 Hz), 120.68 (ArC, $^4J_{CF}$=3.11 Hz), 123.87 (ArC), 125.01 (ArC), 125.18 ($ArC_{[Thio]}$), 127.28 ($ArC_{[Thio]}$), 129.38 ($ArC_{[Thio]}$), 137.25 ($ArC_{Q[Thio]}$), 139.6 (ArC_Q, $^2J_{CF}$=14.53 Hz), 140.94 (CH=$\underline{CH}$–O, J=16.2 Hz), 146.51 (ArC_Q), 151.3 (ArC_Q, $^3J_{CF}$=5.2 Hz), 152.74+156.44 (Ar–F, $^1J_{CF}$=251 Hz), 162.14 (ArC_Q–O), 164.37 (CO_2). $C_{23}H_{21}FN_2O_3S$ expected: C, 65.08%; H, 4.99%; F, 4.48%; N, 6.60%; O, 11.31%; S, 7.55%. CHN found: C, 65.11%; H, 4.9%; N, 6.59%. HRMS (ESCI) 425.1332 (M+H).

3-(Thiophen-3-yl)-acrylic acid 4-(4-*n*-alkoxyphenylazo)-2,3-difluorophenyl esters (series IX; 20a–d). The following spectroscopic data for 3-thiophen-3-yl-acrylic acid 4-(4-*n*-butyloxyphenylazo)-2,3-difluorophenyl ester is representative for the remaining members of series **IX**: ν_{max} (KBr)/cm^{-1}: 3091w (Ar–H_{str}), 2953, 2857w (C–H_{str}), 1733s (C=O_{str}), 1629s (alkene C=C_{str}), 1601, 1498s (C=C_{str}), 1257, 1118s (C–O_{str}), 841s (C–H_{def}, 2 adjacent H); δ_H (270 MHz: $CDCl_3$; Me_4Si) 0.92 (3H, t, CH_3), 1.41 (2H, sext, $CH_3\underline{CH_2}CH_2$–), 1.81 (2H, quint, $\underline{CH_2}$–CH_2–O), 4.01 (2H, t, –$CH_2\underline{CH_2}$OAr), 6.46 (1H, d, $\underline{CH}$=CH–O, J=15.8 Hz), 7.0 (2H,d, ArH), 7.06 (1H, m, ArH), 7.36 (2H, m, $ArH_{[Thio]}$), 7.59 (2H, m, $ArH_{[Thio]}$ and ArH), 7.89 (1H, d, CH=$\underline{CH}$–O, J=15.8Hz), 7.93 (2H, d, ArH); δ_C (67.9 MHz: $CDCl_3$; Me_4Si) 14.07, 22.65, 31.8 ($\underline{CH_2}$–CH_2–O), 68.41 (CH_2–O), 111.7 (ArC_Q, $^4J_{CF}$=4.15), 114.7 (ArC), 116.62 ($\underline{CH}$=CH–O), 118 (ArC_Q, $^4J_{CF}$=4.15 Hz), 125.15 ($ArC_{[Thio]}$), 125.4 (ArC), 127.34 ($ArC_{[Thio]}$), 129.64 ($ArC_{[Thio]}$), 137.12 ($ArC_{Q[Thio]}$), 139.75 (ArC_Q, $^2J_{CF}$=5.2 Hz), 140.6 (ArC_Q, $^2J_{CF}$=10.38 Hz), 140.7 (CH=$\underline{CH}$–O), 141.36–146 (Ar–F, $^1J_{CF}$=238.75 Hz, $^2J_{CF}$=12.45 Hz), 146.9 (ArC_Q), 147.1–150.89 (Ar–F, $^1J_{CF}$=249 Hz, $^2J_{CF}$=11.4 Hz), 162.5 (ArC_Q–O), 163.97 (CO_2). $C_{23}H_{20}F_2N_2O_3S$ expected: C, 62.43%; H, 4.56%; F, 8.59%; N, 6.33%; O, 10.85%; S, 7.25%. CHN found: C, 62.36%; H, 4.58%; N, 6.35%. HRMS (ESCI) 443.1231 (M+H).

3-(Thiophen-3-yl)-acrylic acid 4-(4-*n*-alkoxyphenylazo)-3,5-difluorophenyl esters (series XIII; 22a–d). The following spectroscopic data for 3-thiophen-3-yl-acrylic acid 4-(4-*n*-butyloxyphenylazo)-3,5-difluorophenyl ester is representative for the remaining members of series **XIII**: ν_{max} (KBr)/cm^{-1}: 3102w (Ar–H_{str}), 2927, 2856w (C–H_{str}) 1742s (C=O_{str}), 1629s (alkene C=C_{str}) 1599, 1498s (C=C_{str}), 1251, 1115s (C–O_{str}), 872 (C–H_{def}, 2 adjacent H); δ_H (270 MHz: $CDCl_3$; Me_4Si) 0.92 (3H, t, CH_3), 1.41 (2H, sext, $CH_3\underline{CH_2}CH_2$–), 1.81 (2H, quint, $\underline{CH_2}$–CH_2–O), 4.01 (2H, t, –$CH_2\underline{CH_2}$OAr), 6.52 (1H, d, $\underline{CH}$=CH–O, J=15.8 Hz), 7.0 (2H, d, ArH), 7.37 (2H, m, $ArH_{[Thio]}$), 7.57 (2H, ArH), 7.59 (1H, m, $ArH_{[Thio]}$), 7.88 (2H, d, ArH), 7.89 (1H, d, CH=$\underline{CH}$–O, J=15.8 Hz); δ_C (67.9 MHz: $CDCl_3$; Me_4Si) 14.07, 22.65, 31.8 ($\underline{CH_2}$–CH_2–O), 68.41 (CH_2–O), 106.6 (ArC, $^2J_{CF}$=23.9 Hz), 114.8 (9, ArC and $\underline{CH}$=CH–O), 124.05 (ArC_Q), 125.16 ($ArC_{[Thio]}$), 125.2 (ArC), 127.31 ($ArC_{[Thio]}$), 129.67 ($ArC_{[Thio]}$), 137.14 ($ArC_{Q[Thio]}$), 141.59 (CH=$\underline{CH}$–O), 150.33 (ArC_Q), 150.33 (ArC_Q, $^3J_{CF}$=5.19 Hz), 153.64+157.42 (Ar–F, $^1J_{CF}$=246 Hz, $^3J_{CF}$=5.2 Hz), 162.51 (ArC_Q–O), 163.44 (CO_2). $C_{23}H_{20}F_2N_2O_3S$ expected: C, 62.43%; H, 4.56%; F,

8.59%; N, 6.33%; O, 10.85%; S, 7.25%. CHN found: C, 62.41%; H, 4.52%; N, 6.27%. HRMS (ESCI) 443.1240 (M+H).

3-(Thiophen-3-yl)-acrylic acid 4-(4-*n*-alkoxyphenylazo)-2,6-difluorophenyl esters (series XI; 21a–d). The following spectroscopic data for 3-thiophen-3-yl-acrylic acid 4-(4-*n*-butyloxyphenylazo)-2,6-difluorophenyl ester is representative for the remaining members of series **XI**: ν_{max} (KBr)/cm^{-1}: 3093w (Ar–H_{str}), 2937, 2865w (C–H_{str}), 1730s (C=O_{str}), 1630s (alkene C=C_{str}), 1602, 1498s (C=C_{str}), 1256, 1125s (C–O_{str}), 843s (C–H_{def}, 2 adjacent H); δ_H (270 MHz; $CDCl_3$; Me_4Si) 0.92 (3H, t, CH_3), 1.41 (2H, sext, $CH_3\underline{CH_2}CH_2$–), 1.81 (2H, quint, $\underline{CH_2}$–CH_2–O), 4.01 (2H, t, –$CH_2\underline{CH_2}$OAr), 6.4 (1H, d, $\underline{CH}$=CH–O, J=16 Hz), 6.94 (2H, d, ArH), 7.0 (2H, d, ArH), 7.09 (1H, d, $ArH_{[Thio]}$, H_D, J=5.64 Hz), 7.35 (1H, d, $ArH_{[Thio]}$, H_E, J=3.73 Hz), 7.62 (1H, m, $ArH_{[Thio]}$), 7.88 (1H, d, CH=$\underline{CH}$–O, J=16 Hz), 7.93 (2H, d, ArH); δ_C (67.9 MHz: $CDCl_3$; Me_4Si) 14.07, 22.65, 31.8 ($\underline{CH_2}$–CH_2–O), 68.41 (CH_2–O), 106.7 (ArC, $^2J_{CF}$=27.8 Hz), 114.8 (ArC), 115.85 ($\underline{CH}$=CH–O), 125.13 (ArC), 125.21 ($ArC_{[Thio]}$), 127.5 ($ArC_{[Thio]}$), 129.38 (ArC_Q), 129.8 ($ArC_{[Thio]}$), 137.2 ($ArC_{Q[Thio]}$), 140.25 (CH=$\underline{CH}$–O), 147.69 (ArC_Q), 150.9 (ArC_Q, $^3J_{CF}$=13.42 Hz), 154.68+157.32, (13, Ar–F, $^1J_{CF}$=252.7 Hz, $^3J_{CF}$=7.67 Hz), 162.63 (ArC_Q–O), 1634.14 (CO_2). $C_{23}H_{20}F_2N_2O_3S$ expected: C, 62.43%; H, 4.56%; F, 8.59%; N, 6.33%; O, 10.85%; S, 7.25%. CHN found: C, 62.39%; H, 4.46%; N, 6.3 %. HRMS (ESCI) 443.1232 (M+H).

4-(4-*n*-Alkoxyphenylazo)phenyl cinnamates (series III; 12a–j). The following spectroscopic data for 4-(4-*n*-heptyloxyphenylazo)phenyl cinnamate is representative for the remaining members of Series **III**: ν_{max} (KBr)/cm^{-1}: 3094 w (Ar–H_{str}), 2937, 2855w (C–H_{str}), 1730s (C=O_{str}), 1630s (alkene C=C_{str}), 1602, 1498s (C=C_{str}), 1256, 1125s (C–O_{str}), 843s (C–H_{def}, 2 adjacent H); δ_H (270 MHz: $CDCl_3$; Me_4Si) 0.92 (3H, t, CH_3), 1.35 (8H, m, –$(CH_2)_4$–), 1.82 (2H, quint, $\underline{CH_2}$–CH_2–O), 4.04 (2H, t, $\underline{CH_2}$–O), 6.46 (1H, d, $\underline{CH}$=CH–O, J=15.8 Hz), 7.0 (2H, d, ArH), 7.33 (2H, d, ArH), 7.44 (3H, m, 2H, ArH), 7.61 (2H, t, ArH), 7.87 (1H, d, CH=$\underline{CH}$–O, J=15.8 Hz), 7.91 (2H, d, ArH), 7.3 (2H, d, ArH); δ_C (67.9 MHz: $CDCl_3$; Me_4Si) 14.06, 22.61, 25.7, 29.06, 29.15 ($\underline{CH_2}$–CH_2–O), 31.58 (CH_2), 68.33 (CH_2–O), 114.7 (ArC), 117.02 ($\underline{CH}$=CH–O), 122.16 (ArC), 123.69 (ArC), 124.75 (ArC), 128.34 (ArC), 129.01 (ArC), 130.8 (ArC), 134.07 (ArC_Q), 146.73 (ArC_Q), 146.95 (CH=$\underline{CH}$–O), 150.37 (ArC_Q), 152.23 (ArC_Q), 161.74 (ArC_Q–O), 165.11 (CO_2). $C_{28}H_{30}N_2O_3$ expected: C, 75.99%; H, 6.83%; N, 6.33%; O, 10.85%. CHN found: C, 75.96%; H, 6.76%; N, 6.25%. HRMS (ESCI) 423.2327 (M+H).

2.3. *Polarizing microscopy and transition temperatures*

The mesomorphic transition temperatures were determined by polarizing light microscopy using an Olympus BH2 polarizing microscope in conjunction with a Mettler FP52 hot stage and FP5 control unit. Complementary transition temperatures and their enthalpy values were determined using a Perkin Elmer Diamond differential scanning calorimeter at heating and cooling rates of 10°C min^{-1}. For the initial study of the influence of replacing a benzene ring with either a 2- or 3-substituted thiophene ring, 10 members (n=1–10) of series **I**, **II** and **III** were prepared. Their mesomorphic transition temperatures are listed in Tables 1, 2 and 3, respectively. Similarly, the transition temperatures of members of the fluorinated compounds (series **IV**–**XIII**) are listed in Tables 4–13, respectively. In this instance, the four short homologues (n=1–4) of each series were prepared for better comparative purposes since attempting to compare across several homologues is fraught with difficulties due to changing variables as the homologous series is ascended. For example, it is well known that nematic thermal stability tends to decrease as a homologous series is ascended and there is greater scope for smectic phase formation. The latter may also invoke smectic polymorphism.

All of the homologues of series **I**–**III** (n=1–10) and of series **IV**–**XIII** (n=1–4) are nematogenic. The nematic phase is detected easily on cooling from the isotropic liquid by the appearance of nematic droplets emanating from the isotropic liquid (optically extinct, dark background), which coalesce to give classical threaded and marbled textures.

For the sake of brevity, transition temperature plots are only shown for members of series **I**–**III** (see figures 2–4). Although data points for the I–N transition temperatures are connected point to point with a solid line, classical odd–even behaviour is observed. Even though only four homologues are reported for members of series **IV**–**XIII**, the onset of similar trends is observed.

2.4. *Structure–property relationships*

2.4.1. Influence of altering the nature and disposition of the right-hand terminal aromatic group of the ester. The influence of altering the nature and position of the right-hand terminally disposed aromatic moiety on mesophase type, thermal stability and phase range is summarized in the data displayed in table 14. Irrespective of the terminal aromatic moiety, all of the homologues exhibit the nematic phase. A nematic thermal stability order may be expressed as follows:

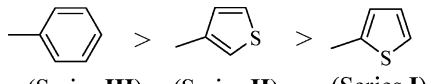

(Series **III**) (Series **II**) (Series **I**)

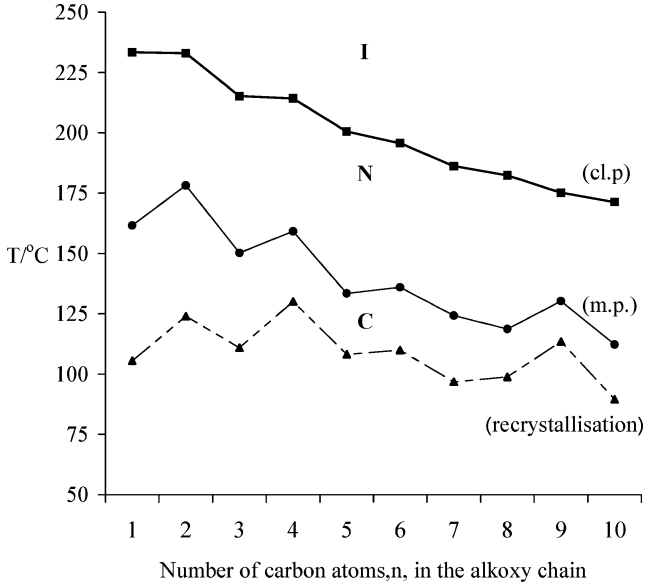

Figure 2. Transition temperature plot for the members of a homologous series of 3-thiophen-2-yl-acrylic acid 4-(4-*n*-alkoxyphenylazo)phenyl esters (series **I**).

demonstrating that replacement of a terminal phenyl moiety (series **III**) with either a 3-thienyl (series **II**) or 2-thienyl moiety (series **I**) reduces the average clearing point ($T_{N–I}$) by 2.7 or 10°C, respectively.

The above nematic mesophase stability order may be related to differences in linearity and subsequent packing of the molecules in the crystal lattice. As expected series **III**, which serves as our control, gives the best thermal stability due to its classical calamitic molecular architecture. Owing to the inherent nature of thiophene, non-linearity reduces the efficiency of packing and thus lowers the mesophase thermal stability of members of series **I** and **II**. Interestingly, it appears that the packing efficiency and intermolecular attractions are stronger for 3-thienyl (series **II**) than 2-thienyl (series **I**), implying a less strained system.

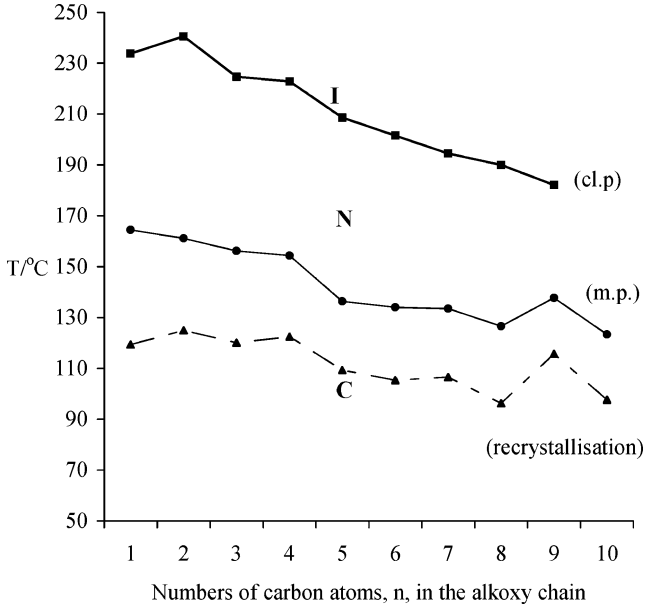

Figure 3. Transition temperature plot for the members of a homologous series of 3-thiophen-3-yl-acrylic acid 4-(4-*n*-alkoxyphenylazo)phenyl esters (series **II**).

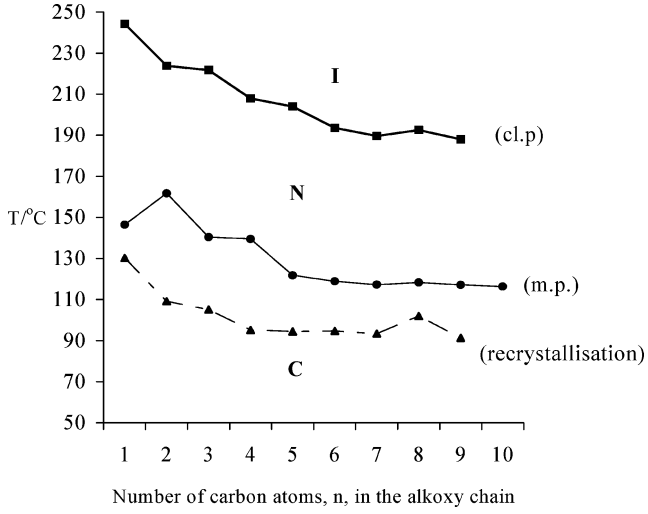

Figure 4. Transition temperature plot for the members of a homologous series of 4-(4-*n*-alkoxyphenylazo)phenyl cinnamates (series **III**).

Likewise, the average phase range ($T_{N–I}$–$T_{C–N}$) shows a similar stability order: phenyl (series **III**)>3-thienyl (series **II**)>2-thienyl (series **I**). In this instance, the change from phenyl to either 3-thienyl or 2-thienyl lowers the phase range by 15.7 or 20.6°C, respectively.

Nabeshima *et al* [14] have reported on the n=4–7 alkyl-substituted analogues of series **I**. A comparison of the influence of alkyl- versus alkoxy-terminal chain on mesomorphic properties is summarized in table 15. Replacement of a methylene unit, –CH_2–, with an

Table 14. Average $T_{N–I}$ (clearing point), $T_{N–I}$–$T_{C–N}$ (phase range) and phase type for n=1–10 homologues of series **I**–**III**.

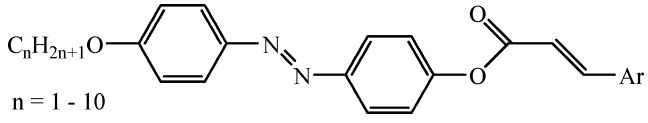

Ar	Average T_{N-I} (°C)	Average $T_{N–I}-T_{C–N}$ (°C)	Phase type
2-Thienyl (series **I**)	202.1	61.7	N
3-Thienyl (series **II**)	209.4	66.6	N
Phen-4-yl (series **III**)	212.1	82.3	N

Table 15. Mesomorphic properties of the n=4–7 homologues of 3-thiophen-2-yl acrylic acid 4-(4-*n*-alkoxyphenylazo)phenyl esters (series **I**) and 3-thiophen-2-yl acrylic acid 4-(4-*n*-alkylphenylazo)phenyl esters (in italics).

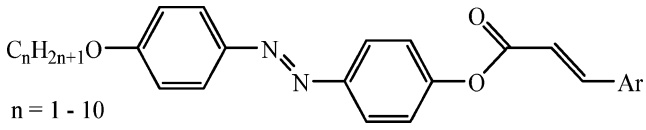

R	C–N	N–I	Phase range
C_4H_9O–	159.2	215.7	56.5
C_4H_9–	*112*	*171*	*59*
$C_5H_{11}O$–	133.0	201.4	67.9
C_5H_{11}–	*113*	*165*	*52*
$C_6H_{13}O$–	136.0	197.8	61.8
C_6H_{13}–	*114*	*157*	*43*
$C_7H_{15}O$–	124.7	187.1	62.4
C_7H_{15}–	*110*	*134*	*24*

oxygen atom increases mesophase thermal stability due to mesomeric relay of the lone pair of electrons on the oxygen atom with the azobenzene central core, increasing the molecular polarizability along the long axis of the molecule.

2.4.2. Influence of introducing lateral fluoro-substituent(s). The influence of introducing lateral fluoro-substituent(s) on mesophase type, thermal stability and phase range is summarized in table 16. As discussed earlier, the four short homologues, n=1–4, from each series have been prepared in order to minimize variables that may be prominent as a homologous series is ascended.

It is now well known that the influence of lateral fluorination on mesophase thermal stability, mesophase range and mesophase type is dependent on the subtle interplay of several factors, namely: the number of lateral fluoro-substituents; the disposition of lateral fluoro-substituents; the association and dissociation of polarity along and across the molecular long axis; and steric crowding [11, 12]. Thus, a clear-cut rationale cannot always be deduced, but instead tentative assumptions are inferred. To extract and rationalize the data listed in table 16 into a meaningful structure–property relationship, it is best to initially review compounds derived from 3-(2-thienyl)acrylic acid (series **I**, **IV**, **VI**, **VIII**, **X** and **XII**), followed by compounds derived from the isomeric 3-(3-thienyl)acrylic acid (series **II**, **V**, **VII**, **IX**, **XI** and **XIII**) and, finally, express an overall mesophase thermal stability order for the complete series of compounds, i.e. series **I**, **II**, **IV**–**XIII**.

2.4.2.1. Influence of lateral fluorination of acrylates derived from 3-(2-thienyl)acrylic acid (series I, IV, VI, VIII, X and XII)

The influence of lateral fluorination on the average mesophase thermal stability ($T_{N–I}$) may be expressed by the stability order shown in figure 5.

A comparison with parent non-fluorinated analogues (series **I**: average $T_{N–I}$ of 225.7°C), reveals that the inclusion of either a monofluoro- or difluoro-substituent(s) decreases the average mesophase thermal

Table 16. Average $T_{N–I}$ (clearing point), $T_{N–I}$–$T_{C–N}$ (phase range) and phase type for homologues n=1–4 of series **I**, **II**, **IV**–**XIII**.

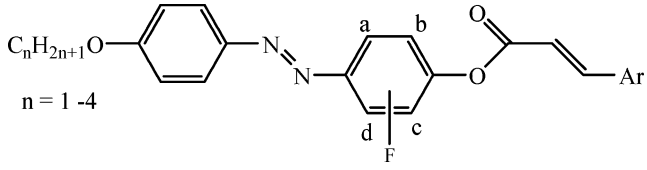

Ar	Series	Position of fluorine(s)	Average $T_{N–I}$ (°C)	Average $T_{N–I}$–$T_{C–N}$ (°C)	Phase type
2-Thienyl	**I**	—	225.7	63.4	N
2-Thienyl	**IV**	a	206.5	61.4	N
2-Thienyl	**VI**	b	208.7	43.2	N
2-Thienyl	**VIII**	a, b	209.6	62.1	N
2-Thienyl	**X**	b, c	190.9	28.8	N
2-Thienyl	**XII**	a, d	192.1	40.8	N
3-Thienyl	**II**	—	232.0	73.1	N
3-Thienyl	**V**	a	210.9	67.5	N
3-Thienyl	**VII**	b	209.3	32.6	N
3-Thienyl	**IX**	a, b	210.9	67.1	N
3-Thienyl	**XI**	b, c	185.0	9.3	N
3-Thienyl	**XIII**	a, d	198.9	53.4	N

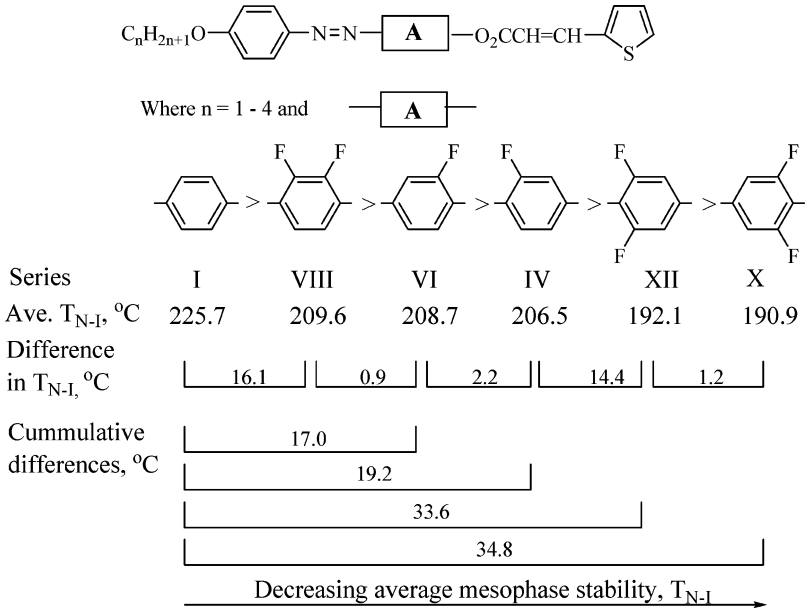

Figure 5. The mesophase stability order for esters derived from 3-(2-thienyl)acrylic acid (series **I**, **IV**, **VI**, **VIII**, **X** and **XII**).

stability. Interestingly, 2,3-difluoro-substitution (series **VIII**: average T_{N-I} of 209.6°C) provides the most stable fluorinated compounds, whereas 2,6-difluoro-substitution (series **X**: average T_{N-I} of 190.9°C) reveals the least thermally stable series. Across-axis substitution appears to be more detrimental to mesophase thermal stability than along the same molecular axis. This may be further exemplified by the flowchart in figure 6, which shows changes in magnitude of the average clearing point

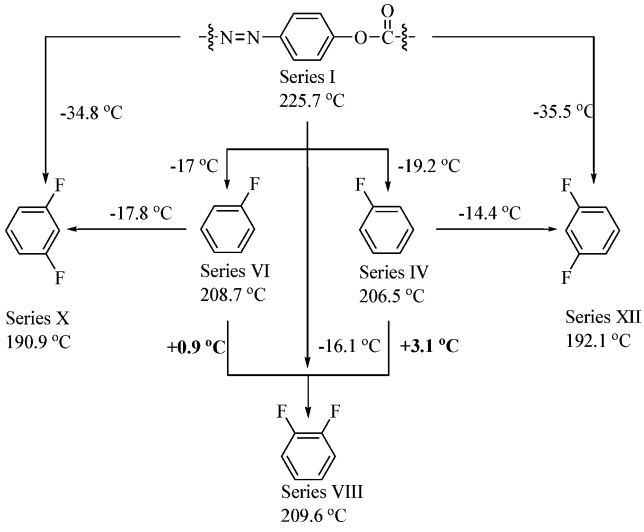

Figure 6. Flowchart showing changes in magnitude of the average clearing point based on the number and disposition of fluoro-substituents for esters derived from 3-(2-thienyl)acrylic acid.

based on the number and disposition of fluoro-substituents.

Compared with the non-fluorinated parent compound (series **I**: average T_{N-I} of 225.7°C), the introduction of a monofluoro-substituent either on an *outer edge* (series **VI**: *ortho*- to the $-O_2C-$ linkage and *meta*- to the azo linkage) or an *inner edge* (series **IV**: *ortho*- to the $-N=N-$ linkage and *meta*- to the $-O_2C-$ linkage) lowers the thermal stability by 17 and 19.2°C, respectively. The lateral fluoro-substituent increases the molecular breadth and its disposition does not seem to be too significant as only a minor difference in mesophase thermal stability between the two monofluoro-substituted isomers is detected, i.e. between series **VI** (average T_{N-I} of 208.7°C) and series **IV** (average T_{N-I} of 206.5°C).

However, the influence of introducing a second lateral fluoro-substituent on mesophase thermal stability is dependent on the initial disposition of the first fluoro-substituent and its inclusion thereafter, i.e. either on the same side (series **VIII**) or across the molecular long axis (series **X** or **XII**). The introduction of a second fluoro-substituent across the molecular axis in series **VI** (average T_{N-I} of 208.7°C) to generate series **X** (average T_{N-I} of 190.9°C) lowers the thermal stability by 17.8°C. A similar trend is observed when a second across-axis fluoro-substituent is introduced in series **IV** (average T_{N-I}, 206.5°C) generating series **XII** (average T_{N-I} of 192.1°C) revealing a decrease in thermal stability of 14.4°C. The drop in thermal stability by approximately 16°C (average of 17.8 and 14.4°C) merely reflects a

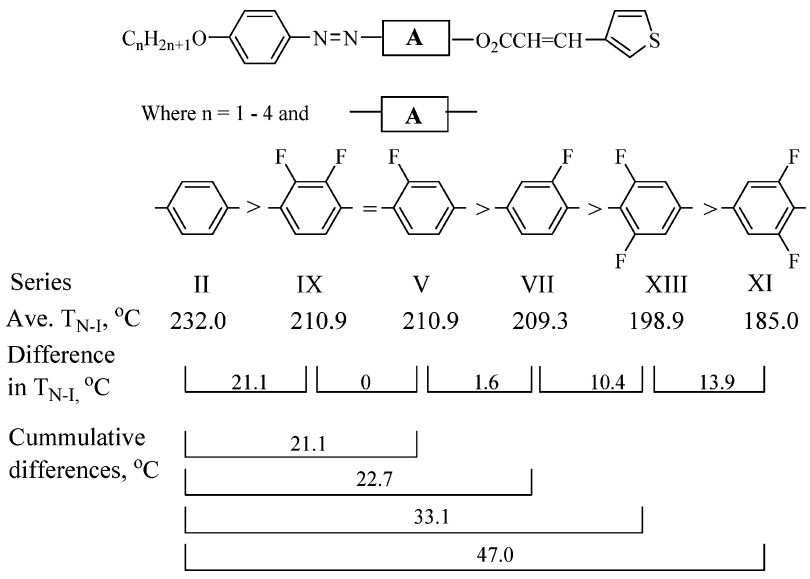

Figure 7. The mesophase stability order for esters derived from 3-(3-thienyl)acrylic acid (series **II**, **V**, **VII**, **IX**, **XI** and **XIII**).

further increase in lateral broadening and inter-annular twisting. The latter will be evident at either end of the phenyl ring as one end is attached to –N=N– and the other to $–O_2C–$.

The introduction of a second fluoro-substituent on the same side of the molecular long axis (adjacent to initial fluoro-substituent), i.e. series **VIII**, maintains or slightly enhances the mesophase thermal stability. A progressive increase in lateral fluorination does not always lower mesophase thermal stability as demonstrated by going from either series **IV** or **VI** to series **VIII**. The introduction of a second lateral substituent to series **VI** (average $T_{N–I}$ of 208.7°C) to obtain series **VIII** (average $T_{N–I}$ of 209.6°C) nominally increases the thermal stability by 0.9°C. The second fluoro-substituent in this case demonstrates a space-filling effect. However, the inclusion of a second lateral substituent to series **IV** (average $T_{N–I}$ of 206.5°C) to give series **VIII**

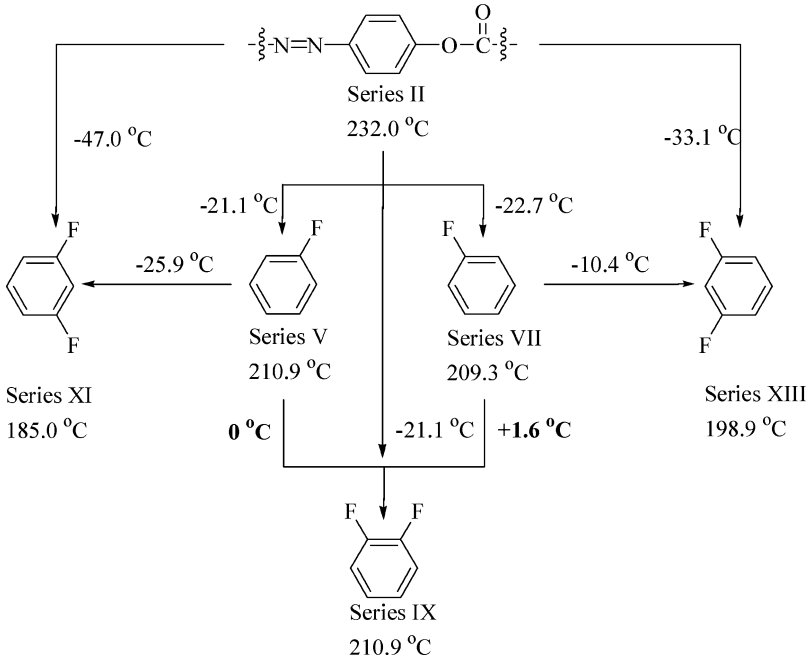

Figure 8. Flowchart showing the influence of increasing the number of lateral fluoro-substituents on mesophase thermal stability for esters derived from 3-(3-thienyl)acrylic acid.

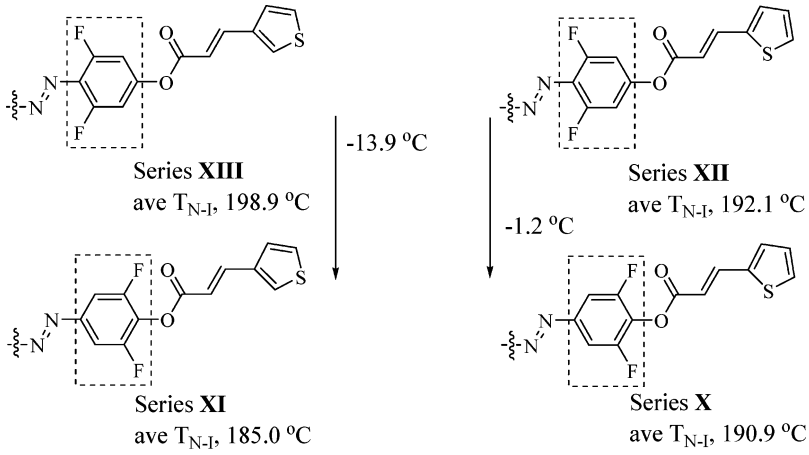

Figure 9. Summary of the effect of the two across-axis fluoro-substituents in relation to the disposition of the thiophene ring on average mesophase stability.

(average T_{N-I} of 209.6°C) enhances the thermal stability by 3.1°C suggesting an enhancement of polar electronic effects or better conformational ordering of the molecule.

2.4.2.2. Influence of lateral fluorination of acrylates derived from 3-(3-thienyl)acrylic acid (Series II, V, VII, IX, XI ***and*** *XIII)*

The mesophase stability order shown in figure 7 for esters derived from 3-(3-thienyl)acrylic acid (series **II**, **V**, **VII**, **IX**, **XI** and **XIII**) is noticeably different from the order shown by their isomeric counterparts derived from 3-(2-thienyl)acrylic acid (i.e. series **I**, **IV**, **VI**, **VIII**, **X** and **XIII**), implying a strong dependency on both the disposition of the terminal thienyl moiety and the fluoro-substituent.

As shown by the flowchart in figure 8, which maps the influence of increasing the number of lateral fluoro-substituents on mesophase thermal stability, the inclusion of a monofluoro-substituent on an inner edge (series **V**: average T_{N-I} of 210.9°C) decreases the thermal stability by 21.1°C, whereas on an outer edge (series **VII**: average T_{N-I} of 209.3°C) thermal stability decreases by 22.7°C. The magnitude of decrease in thermal stability is more than for their isomeric counterparts derived from 3-(2-thienyl)acrylic acid, i.e. series **IV** and **VI**. There is a nominal difference of 0.6°C in thermal stability between series **V** and **VII**. The inclusion of a second fluoro-substituent on the same side of the molecular axis in series **V** to obtain series **IX** exemplifies a 'perfect space-fill effect' where no change in thermal stability is observed. Both series **IX** and **V** have the same thermal stability (average T_{N-I} of 210.9°C) and represent the most stable of the fluorinated compounds. An enhancement of thermal stability by 1.6°C is detected when a second fluoro-substituent

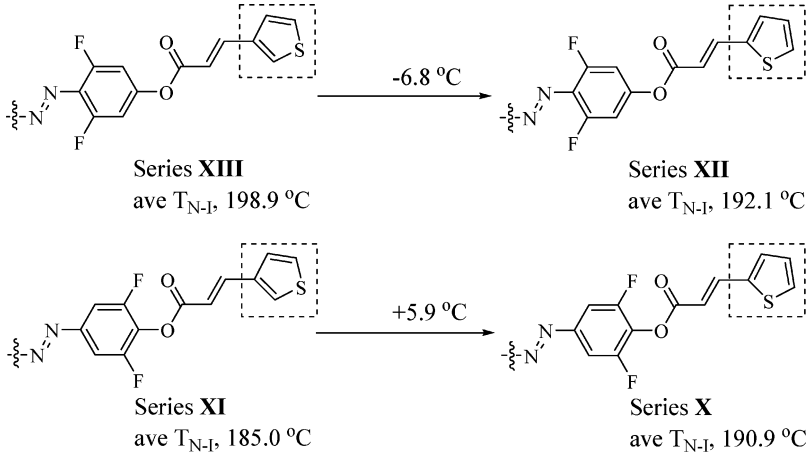

Figure 10. Summary of the influence of the disposition of the terminal thiophene when the across-axis fluoro-substituents are fixed.

adjacent to the first is introduced in series **VII**. There appears to a be synergistic effect between the fluoro-substituent and the ester linkage similar to that observed for the isomeric 3-(2-thienyl)acrylyl-derived compounds which showed an increase of 3.1°C (series **IV**–**VIII**).

Again, across-axis difluoro-substitution is more detrimental to mesophase thermal stability than along the long molecular axis. The inclusion of a second *outer edge* fluoro-substituent in series **V** (average T_{N-I} of 210.9°C) to obtain series **XI** (average T_{N-I} of 185.0°C) decreases the thermal stability by 25.9°C. However, the inclusion of a second *inner edge* fluoro-substituent in series **VII** (average T_{N-I} of 209.3°C) to yield series **XIII** (average T_{N-I} of 198.9°C) is less detrimental and a decrease of 10.4°C is observed.

The disposition of the two across-axis fluoro-substituents in relation to the disposition of the thiophene ring is summarized in figure 9. If the thiophene moiety is *fixed*, then *outer edge* di-substitution is more detrimental than *inner edge* di-substitution. For example, both series **XIII** and **XII** are more thermally stable than series **XI** and **X** by 13.9 and 1.2°C, respectively.

Alternatively, if the across-axis fluoro-substituents are *fixed*, then the influence of the disposition of the terminal thiophene may be investigated as highlighted in figure 10.

When the fluoro-substituents are located on an *inner edge*, the 3-(3-thienyl)acrylyl-derived compounds (series **XIII**: average T_{N-I} of 198.9°C) are 6.8°C more stable than their 3-(2-thienyl)acrylyl counterparts (series **XII**: average T_{N-I} of 192.1°C). However, the opposite is observed when the fluoro-substituents are located on an *inner edge*. The 3-(3-thienyl)acrylyl-derived compounds (series **XI**: average T_{N-I} of 185.0°C) are 5.9°C less stable than the 3-(2-thienyl)acrylyl counterparts (series **X**: average T_{N-I} of 190.9°C). The disposition of the thiophene ring does play an important role in mesophase thermal stability, either showing enhancement or destabilization.

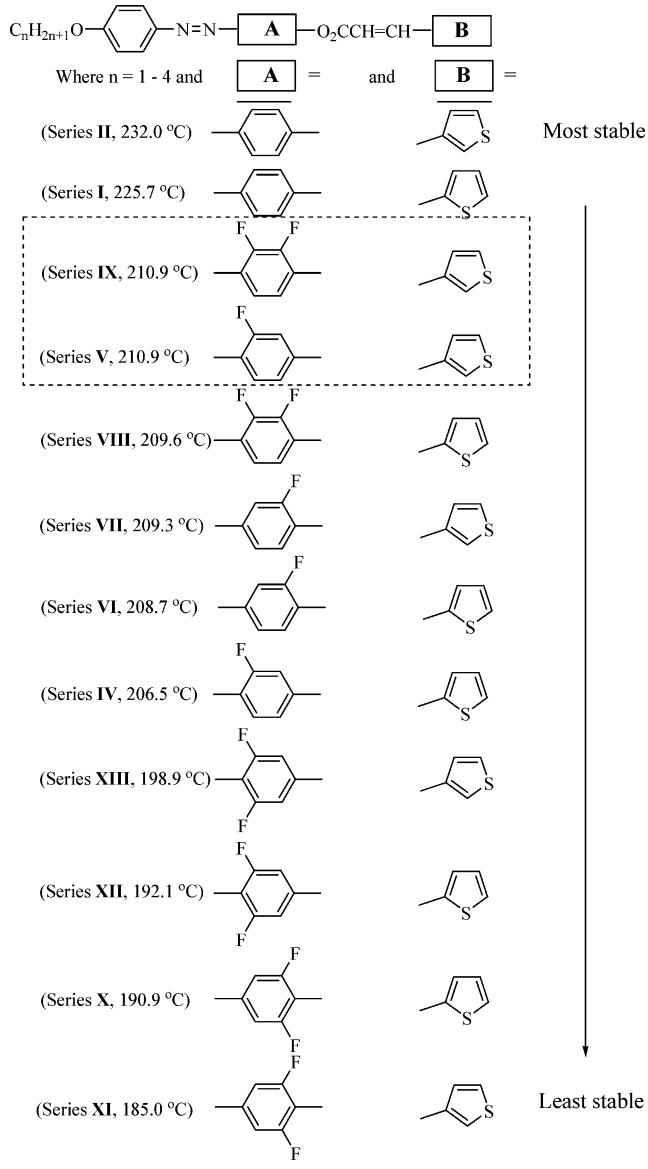

Figure 11. Influence of varying the number and disposition of lateral fluoro-substituents in a variety of esters derived from either 3-(2-thienyl)acrylic acid (series **I**, **IV**, **VI**, **VIII**, **X** and **XII**) or 3-(3-thienyl)acrylic acid (series **II**, **V**, **VII**, **IX**, **XI** and **XIII**) on the average mesophase thermal stability.

2.5. *Summary of structure–property relationships*

The influence of varying the number and disposition of lateral fluoro-substituents in a variety of esters derived from either 3-(2-thienyl)acrylic acid (series **I**, **IV**, **VI**, **VIII**, **X** and **XII**) or 3-(3-thienyl)acrylic acid (series **II**, **V**, **VII**, **IX**, **XI** and **XIII**) on the average mesophase thermal stability is summarized in figure 11. The order clearly shows that lateral fluorination lowers the mesophase thermal stability with respect to the parent non-fluorinated analogues. Difluoro-substitution on the same side of the molecular long axis is less detrimental to mesophase thermal stability than difluoro-substitution across the molecular long axis. The disposition of the terminal thienyl moiety also effects mesophase thermal stability, either by enhancement or destabilization.

References

[1] D. Vorländer. *Kristallinisch-flussige Substanzen*. Enke, Stuttgart (1908).

[2] D. Vorländer. *Berichte der Deutschen Chemischen Gesellschaft*, **41**, 2033 (1908).

[3] R. Brettle, D.A. Dunmur, C.M. Marson, M. Pinol, K. Toriyama. *Liq. Cryst.*, **13**, 515 (1993).
[4] R. Brettle, D.A. Dunmur, C.M. Marson, M. Pinol, K. Toriyama. *Chem. Lett.*, **21**, 613 (1992).
[5] H. Schubert, I. Sagitidinov, J.V. Svetkin. *Z. Chem.*, **13**, 222 (1975).
[6] J.L. Butcher, D.J. Byron, A.S. Matharu, R.C. Wilson. *Liq. Cryst.*, **19**, 693 (1995).
[7] J.D. Bunning, J.L. Butcher, D.J. Byron, A.S. Matharu, R.C. Wilson. *Liq. Cryst.*, **19**, 387 (1995).
[8] D.J. Byron, L. Komitov, A.S. Matharu, I. McSherry, R.C. Wilson. *J. Mater. Chem.*, **6**, 1871 (1996).
[9] A.S. Matharu, C. Grover, L. Komitov, G. Andersonn. *J. Mater. Chem.*, **10**, 1303 (2000).
[10] A.S. Matharu, S.J. Cowling, G. Wright. *Liq. Cryst.*, **34**, 489 (2007).
[11] G.W. Gray, M. Hird, D. Lacey, K.J. Toyne. *J. Chem. Soc. Perkin Trans. II*, 2041 (1989).
[12] G.W. Gray, M. Hird, D. Lacey, K.J. Toyne. *Mol. Cryst. Liq. Cryst.*, **172**, 165 (1989).
[13] M. Irie. *Chem. Rev.*, **100**, 1683 (2000).
[14] Y. Nabeshima, A. Shishido, A. Kanazawa, T. Shiono, T. Ikeda, T. Hiyama. *Chem. Mater.*, **9**, 1480 (1997).
[15] A. Hassner, V. Alexanian. *Tetrahedron Lett.*, **46**, 4475 (1978).
[16] C. Weygand, R. Gabler. *J. Prakt. Chem.*, **155**, 322 (1940).
[17] R. Nodzu, H. Watanabe, S. Kuwata, C. Nagaishi, T. Terematsu. *Yakugaku Zasshi*, **74**, 872 (1954).